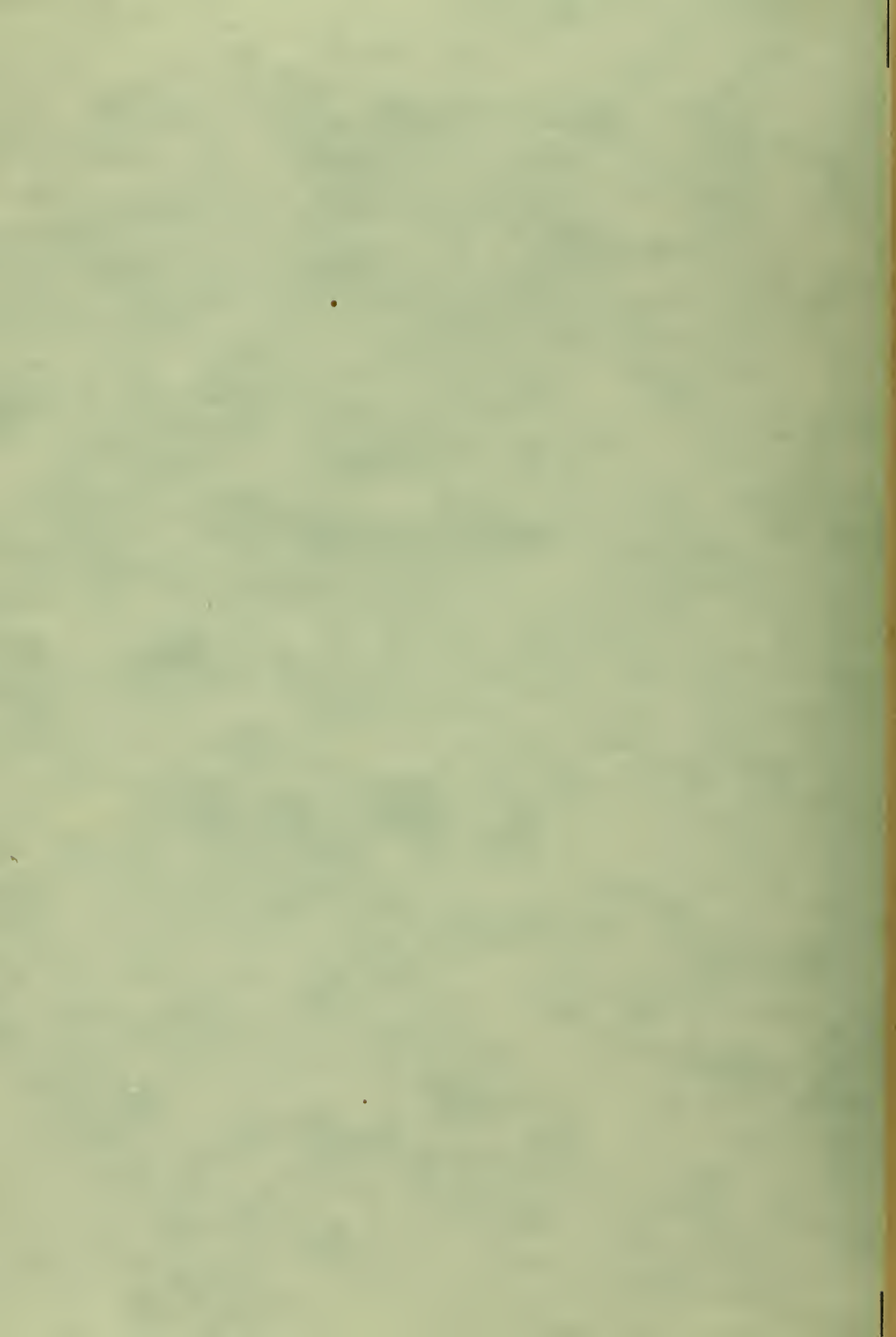


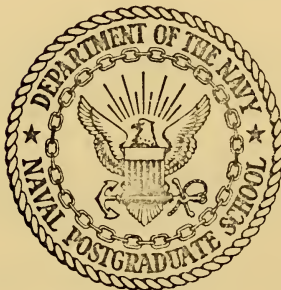
SUBSONIC LIFTING SURFACE ANALYSIS  
WITH STATIC AEROELASTIC EFFECTS

Larry Glen Pearson



# NAVAL POSTGRADUATE SCHOOL

Monterey, California



## THESIS

SUBSONIC LIFTING SURFACE ANALYSIS  
WITH STATIC AEROELASTIC EFFECTS

by

Larry Glen Pearson

Thesis Advisor:

L. V. Schmidt

June 1972

*Approved for public release; distribution unlimited.*



Subsonic Lifting Surface Analysis  
with Static Aeroelastic Effects

by

Larry Glen Pearson  
Lieutenant, United States Navy  
B.S., Naval Postgraduate School, 1971

Submitted in partial fulfillment of the  
requirements for the degree of

MASTER OF SCIENCE IN AERONAUTICAL ENGINEERING

from the

NAVAL POSTGRADUATE SCHOOL  
June 1972

Thesis

p 813

C-1

## ABSTRACT

A computer program was coded to obtain static aeroelastic effects on simple planforms through the use of subsonic lifting surface theory. The program was divided into two major technical areas, aerodynamic and structural, with matrix notation used to indicate the influence of each in the final aerodynamic loading distribution. Several typical stability derivatives were then obtained to make an accurate stability and control analysis on the desired planform.





## TABLE OF CONTENTS

|                           |  |       |    |
|---------------------------|--|-------|----|
| I.                        | INTRODUCTION   | ----- | 9  |
| II.                       | METHODS USED   | ----- | 12 |
| A.                        | GENERAL  | ----- | 12 |
| B.                        | AERODYNAMICS OF THE PROBLEM                                | ----- | 13 |
| C.                        | COMPRESSIBILITY CORRECTIONS FOR<br>SUBSONIC FLOW           | ----- | 19 |
| D.                        | STRUCTURAL ASPECT OF THE PROBLEM                           | ----- | 20 |
| E.                        | TOTAL SOLUTION   | ----- | 21 |
| F.                        | CALCULATION OF STABILITY DERIVATIVES                       | ----- | 22 |
| III.                      | RESULTS AND DISCUSSION                                     | ----- | 26 |
| A.                        | LONGITUDINAL   | ----- | 26 |
| B.                        | LATERAL  | ----- | 29 |
| IV.                       | CONCLUSIONS AND RECOMMENDATIONS                            | ----- | 35 |
| APPENDIX A.               | ASSUMPTIONS  | ----- | 36 |
| APPENDIX B.               | DERIVATION OF THE AERO SUBROUTINE                          | ----- | 37 |
| APPENDIX C.               | DERIVATION OF THE STRUCTURES SUBROUTINE                    | ---   | 43 |
| APPENDIX D.               | TWO-DIMENSIONAL WING PRESSURE LOADING<br>CONVERGENCE CHECK | ----- | 50 |
| COMPUTER PROGRAMS         | -----  | 54    |    |
| REFERENCES                | -----  | 71    |    |
| INITIAL DISTRIBUTION LIST | -----  | 72    |    |
| FORM DD 1473              | -----  | 73    |    |



# TABLE OF FIGURES

|     |  |    |
|-----|--|----|
| 1.  | Horseshoe vortex lattice geometry -----  | 14 |
| 2.  | Finite vortex element, between A and B, of strength $\Gamma$ -----   | 14 |
| 3.  | Contour encircling all $\Gamma$ 's located at the individual boxes -----   | 17 |
| 4.  | Effects of planform distortion -----   | 17 |
| 5.  | Angle of attack distribution for a constant rolling velocity p -----   | 25 |
| 6.  | Ailerons as defined by horseshoe vortices -----  | 25 |
| 7.  | Lift-curve slope and moment-curve slope plotted as a function of leading edge sweep at a Mach number of 0.5 -----            | 27 |
| 8.  | Lift-curve slope and moment-curve slope plotted as a function of Mach number with a leading edge sweep of 20.0 deg -----     | 28 |
| 9.  | Static margin indicator plotted as a function of leading edge sweep at a Mach number of 0.5 -----                            | 30 |
| 10. | Rolling moment due to aileron deflection plotted as a function of free stream dynamic pressure at a Mach number of 0.5 ----- | 32 |
| 11. | Damping in roll derivative plotted as a function of free stream dynamic pressure at a Mach number of 0.5 -----               | 33 |
| 12. | Bending and torsion stiffness curves -----   | 34 |
| B1. | Simplified horseshoe vortices system for wing lift distribution -----  | 38 |
| B2. | Geometry for downwash velocity calculation -----   | 38 |
| C1. | Elastic axis representation of the wind with the torques and moments at the station elastic axis points -----                | 44 |
| D1. | Geometry for two-dimensional study of chordwise pressure distribution -----  | 51 |
| D2. | A tabulation of the two-dimensional wing convergence check -----   | 53 |



# TABLE OF SYMBOLS

|                    |  |
|--------------------|--|
| [A]                | aerodynamic influence-coefficient matrix   |
| [AS]               | symmetric aerodynamic influence-coefficient matrix   |
| [AA]               | anti-symmetric aerodynamic influence-coefficient matrix  |
| $A_n$              | Fourier coefficients for chordwise collocation technique   |
| $\alpha_o$         | lift curve slope of section of infinite wing   |
| $\mathcal{R}$      | wing aspect ratio = $b^2/s$  |
| $B_n$              | Fourier coefficients for spanwise collocation technique  |
| $b$                | wing span  |
| $C$                | planform chord   |
| $\overline{C}$     | wing aerodynamic chord = $\frac{1}{S} \int_{-b/2}^{b/2} c^2 dy$  |
| $C_{ave}$          | average chord of the planform = $s/b$  |
| $C_L$              | total wing lift coefficient, Lift/ $qS$ (+ acts upward)  |
| $C_m$              | total wing pitching moment referenced to $\overline{C}/4$ (pitching moment)/ $qS\overline{C}$ (positive leading edge up) |
| $C_{L\alpha}$      | total wing lift curve slope, $\partial C_L / \partial \alpha$  |
| $C_{m\alpha}$      | static stability derivative, $\partial C_m / \partial \alpha$  |
| $C_{mC_L}$         | indicator for static margin, $C_{m\alpha} / C_{L\alpha}$   |
| $C_{\ell_P}$       | roll damping derivative, $\partial C_{\ell} / \partial (\frac{Pb}{2V})$  |
| $C_{\ell\delta_a}$ | rolling moment due to aileron deflection, $\partial C_{\ell} / \partial \delta_a$  |
| $C_t$              | tip chord  |



|                                       |   |
|---------------------------------------|---|
| $C_r$                                 | root chord  |
| $C_{m_{c/4}}$                         | section pitching moment coefficient about the local quarter chord         |
| $C_l$                                 | section lift coefficient  |
| $C_{l_\alpha}$                        | section lift curve slope  |
| $h$                                   | horseshoe vortex semispan   |
| $l$                                   | section lift  |
| $\left\{ \frac{\Delta l}{q} \right\}$ | incremental aerodynamic loadings over the planform                        |
| $M_\infty$                            | free stream Mach number   |
| NC                                    | number of chordwise stations  |
| NS                                    | number of spanwise stations   |
| N                                     | total number of stations on the planform                                  |
| $P$                                   | rolling velocity (radians per second) ( + right wing going down)          |
| $\frac{pb}{2V}$                       | roll helix angle  |
| $q$                                   | free stream dynamic pressure, a scalar constant $= \frac{1}{2} \rho V^2$  |
| $R_A$                                 | distance from a control point to the left corner of the horseshoe vortex  |
| $S$                                   | structural influence-coefficient matrix                                   |
| $S$                                   | wing area   |
| $V$                                   | free stream velocity  |
| $\Delta w$                            | incremental downwash velocity, (+ acts downward)                          |
| $\left\{ \frac{w}{V} \right\}_{3c/4}$ | distribution of downwash angles at the three-quarter chord control points |
| $x$                                   | axial coordinate  |
| $y$                                   | spanwise coordinate   |





|             |  |
|-------------|--|
| $z$         | vertical coordinate  |
| $\alpha$    | angle of attack (positive is nose up rotation)   |
| $\alpha_f$  | final angle of attack  |
| $\alpha_r$  | rigid input angle of attack  |
| $\alpha_s$  | angle of attack due to structural twist  |
| $\alpha_g$  | geometric angle of attack  |
| $\beta$     | Prandtl-Glauert planform distortion factor, $1/\sqrt{1-M_\infty^2}$                          |
| $\lambda$   | scaling parameter = $\frac{b \text{ prototype}}{b \text{ model}} = (b/2)_{\text{prototype}}$ |
| $\Gamma$    | vortex strength  |
| $\Gamma/V$  | aerodynamic loading  |
| $\phi$      | flow velocity potential  |
| $\phi_{xx}$ | the second partial derivative of $\phi$ with respect to $x$                                  |
| $\rho$      | air density  |
| $\nabla^2$  | Laplacian operator   |

Matrix notation:

|              |                            |
|--------------|----------------------------|
| $[ \ ]$      | rectangular matrix         |
| $[ \ ]$      | row matrix                 |
| $\{ \}$      | column vector              |
| $[ \ ]$      | square diagonal matrix     |
| $[ \ ]^{-1}$ | inverse of a square matrix |



## ACKNOWLEDGEMENT

My most sincere appreciation to Professor L. V. Schmidt for his unending patience and professional guidance.



## I. INTRODUCTION

In making a stability and control analysis on modern high performance aircraft, the ability to make span load evaluations on the wing and tail with static aeroelastic effects taken into account is most important. It seemed desirable to develop a simple computer program utilizing current 'state-of-the-art' theories, and proper documentation, so that design groups might have readily usable methods at hand.

Span load determinations have gone through a long line of evolution, right up to the lifting surface theories of today. Prandtl's lifting line theory is considered as the earliest, which was suitable for simple planforms of high aspect ratio and unswept quarter chords operating in incompressible flow. Modifications of this method were made by Glauert, Multhopp, Weissinger, and others until the present lifting surface theories suitable for low (or high) aspect ratio planforms with swept quarter chords operating in compressible flow were attained.

Two lifting surface concepts for subsonic calculations are:

1. Define the surface pressure loading in the chordwise and spanwise directions by admissible sets of orthogonal functions with the magnitudes of the unknown coefficients being obtained by collocation techniques, Ref. 6.
2. Define a grid of boxes over the wing, each of which contains a horseshoe vortex, Ref. 4. Then determine the strengths



of the vortices by imposing the constraint of flow tangency at an equal number of control points.

The approach chosen for this study was the second, which is usually denoted as a vortex lattice method and is thoroughly described by Belotserkovskii, Ref. 4. The major advantage to this approach is the convenient use of matrix methods for taking the static aero-elastic effects into account.

The method of Gray and Schenk, Ref. 1, used initially on the Boeing B-52 aircraft, was carefully reviewed as background for this study. Their analysis, which was restricted to aspect ratio wings of greater than five, employed the Weissinger L-Method to account for subsonic aerodynamics. The advantage of the lifting surface theory used for this study is that wings of lower aspect ratio may be analyzed and the ability to more accurately predict chordwise (as well as spanwise) distribution of aerodynamic loading is provided. The method of Ref. 1 did not allow for aerodynamic loadings other than additional type,<sup>1</sup> whereas the method of this study is not restricted to loadings with the aerodynamic centers at the local quarter chord.

To account for compressibility in subsonic flow the Prandtl-Glauert rule was used, Ref. 2, sometimes referred to as planform

---

<sup>1</sup> Additional type pressure loadings are defined as the air loadings due to angle of attack only. Generally they have a cotangent type chordwise pressure distribution in subsonic flow with a logarithmic type singularity at the leading edge, and vanish at the trailing edge to satisfy the Kutta condition.





distortion. The aeroelastic effects will depend upon the original wing structure and will vary proportionally with the free stream dynamic pressure. The span load evaluation at zero dynamic pressure corresponds to the rigid wing results. Symmetric span loads will be applicable to longitudinal stability and control analyses, with anti-symmetric to lateral-directional.

The program has been restricted to simple planforms with straight taper, and the influence of fuselage interference was not taken into account. This was not an oversight but deliberate since it was felt appropriate at this time to obtain a straight-forward documentation on a simple wing situation, with applications to more complex planforms and interference effects as a logical extension of this study.

The approach used in the structural area was restricted to a basic beam-like wing structure, corresponding to modelling the wing by an elastic axis with variable stiffness properties along the span for both bending and torsional moments. An influence coefficient concept for plate-type lifting surface might be a more general approach, but this was not felt warranted without a specific application in mind.

The purpose of this study was to develop and document a simple approach for static aeroelastic analysis and airframe stability and control considerations. This documentation is a necessary prelude to more serious considerations on actual configurations such as new current Navy aircraft like the F-14 and S-3.



## II. METHODS USED

### A. GENERAL

In a static aeroelastic analysis there are two distinct technical areas requiring attention. Both the aerodynamics of the problem and the structural aspect must be considered.

With the free-stream subsonic Mach number and dynamic pressure given, the aerodynamic loadings of the rigid wing are given as:

$$[A] \left\{ \frac{\Delta l}{q} \right\} = \{ \alpha_r \} \quad (.01)$$

where  $[A]$  = Aerodynamic influence coefficient matrix at the given Mach number.

$\left\{ \frac{\Delta l}{q} \right\}$  = incremental loadings over the wing.

$\{ \alpha_r \}$  = rigid wing input angle of attack, specified at the control stations.

Structural deformations on the wing due to the aerodynamic loadings result in a change in the angle of attack.

$$q[S] \left\{ \frac{\Delta l}{q} \right\} = \{ \alpha_s \} \quad (.02)$$

where  $q$  = the free stream dynamic pressure, scalar constant.

$[S]$  = the structural influence coefficient matrix.

$\{ \alpha_s \}$  = the angular deflections at the specified control points on the wing due to aerodynamic loadings.



Now the complete solution to the aeroelastic problem is given by:

$$[A] - q[S] \left\{ \frac{\Delta l}{q} \right\} = \{\alpha_r\} \quad \text{---} \quad (.03a)$$

or

$$\left\{ \frac{\Delta l}{q} \right\} = [A] - q[S]^{-1} \{\alpha_r\} \quad \text{---} \quad (.03b)$$

## B. AERODYNAMICS OF THE PROBLEM

The basic approach used in this development is similar to the lifting surface analysis as described by Belotserkovskii Ref. 4.

With the concept of a vortex lattice array of horseshoe vortices the wing is covered with N boxes where:

$$N = NC \times NS \text{-----} (.04)$$

and

NC = Number of chordwise station

NS = Number of spanwise station

In a manner similar to lifting line theory, as developed by Prandtl, Glauert, Multhopp, and Weissinger (Refs. 2 and 3), the swept bound horseshoe vortices were placed at the local quarter chord of each box and the flow tangency requirement imposed at the local three-quarter chord control point of each box. Figure 1 shows the geometry of the problem, with A and B denoting the left- and right-hand corners of the horseshoe vortex element and C the control point.

As a consequence of the Helmholtz vorticity theorems (Ref. 2), and because inviscid flow was assumed, each horseshoe vortex element has constant strength, once established. The Biot-Savart Law



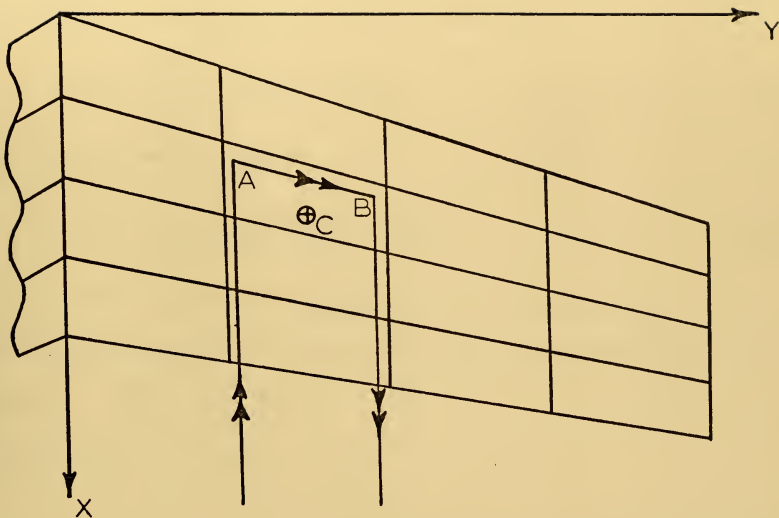


Figure 1. Horseshoe vortex lattice geometry.

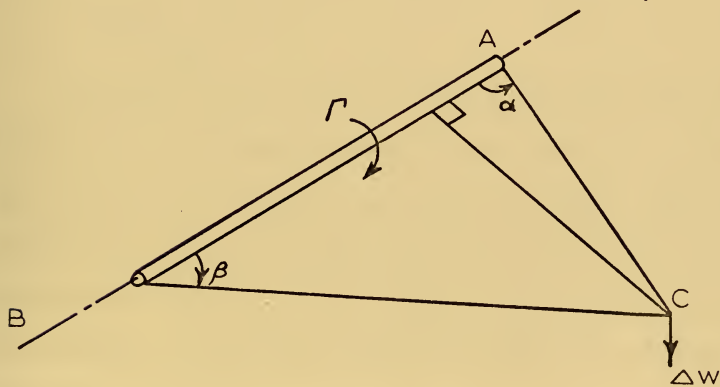


Figure 2. Finite vortex element, between A and B, of strength  $\Gamma$ .





(Ref. 2) then defines the velocity induced at a control station C (see fig. 2), for a vortex filament of finite length as:

$$\Delta \omega = \frac{\Gamma}{4\pi r} (\cos \alpha + \cos \beta) \quad \text{---} \quad (.05a)$$

and the downwash angle as:

$$\frac{\Delta \omega}{V} = \frac{1}{4\pi r} \left( \frac{\Gamma}{V} \right) (\cos \alpha + \cos \beta) \quad \text{---} \quad (.05b)$$

If the vortex element is expanded to plus and minus infinity, the well known expression for downwash angle in two-dimensional flow

results: 
$$\frac{\Delta \omega}{V} = \frac{1}{2\pi r} \left( \frac{\Gamma}{V} \right) \quad \text{---} \quad (.06)$$

since  $\cos \alpha = \cos \beta = 1.0$

As previously stated, the flow tangency requirement was applied at the three-quarter chord control point, and the flow was required to be parallel to the zero lift line at that point. Hence,

$$\left( \frac{\omega}{V} \right)_{3c/4} = \alpha_f \quad (.07)$$

Justification for the use of a local three-quarter chord control point in each vortex lattice box has not been rigorously established. The concept of the "rearward" aero-center at the wing three-quarter chord control point, from steady and unsteady two-dimensional wing aerodynamics, appears to be the genesis of this usage. At present the modelling is considered satisfactory because the theoretical loadings are in accord with experimental results. It is not clear as of this writing why the preservation of flow tangency at local vortex-box three-quarter-chord control points preserves the Kutta condition



at the wing trailing edge, but the calculated values of local vortex box loadings do show the preservation of this trait. (Ref. Appendix D)

The value of the downwash angle  $\left(\frac{\omega}{V}\right)_{\frac{3c}{4}}$  varies at each control station on the wing, and there are contributions by the bound and trailing vortices from all of the wing stations. Hence, the flow tangency requirement may be expressed as a column vector as follows:

$$\left\{\frac{\omega}{V}\right\}_{\frac{3c}{4}} = [A] \left\{\frac{\Gamma}{V}\right\} = [A] \left\{\frac{\Delta\gamma}{q}\right\} \quad \text{---} \quad (.08)$$

where the matrix  $[A]^*$  is the aerodynamic influence-coefficient matrix as developed in Appendix B.

For the vortex lattice representation with N horseshoe vortices, the flow tangency requirement was given by:

$$\begin{aligned} \left\{\frac{\omega}{V}\right\}_{\frac{3c}{4}} &= [A] \left\{\frac{\Delta\gamma}{q}\right\} = \{\alpha_f\} \\ \text{or} \quad \left\{\frac{\Delta\gamma}{q}\right\} &= [A]^{-1} \{\alpha_f\} \quad \text{---} \quad (.09) \end{aligned}$$

There was a temptation to view the vortex strength at each control box as the pressure differential of that box. This, however, is not the case. Again as a result of the Helmholtz vorticity theorems (Ref. 2), the vortex strengths of the individual boxes may be summed in the chordwise direction to obtain the total vorticity at each spanwise station. Hence the vortex strength of a section may be "lumped" into one vortex equal to the sum of the individual vortices. (See Fig. 3.)

---

\*The development of the  $[A]$  matrix for spanwise stations only may be seen in Ref. 1.



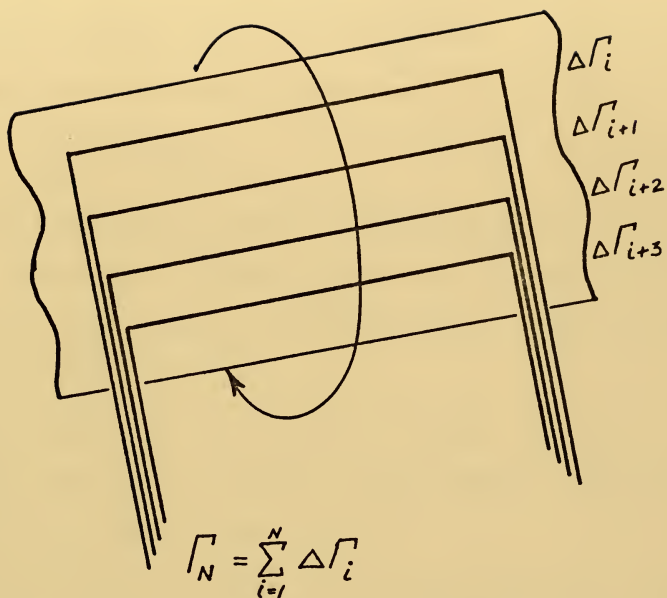


Figure 3. Contour encircling all  $\Gamma$ 's located at the individual boxes.

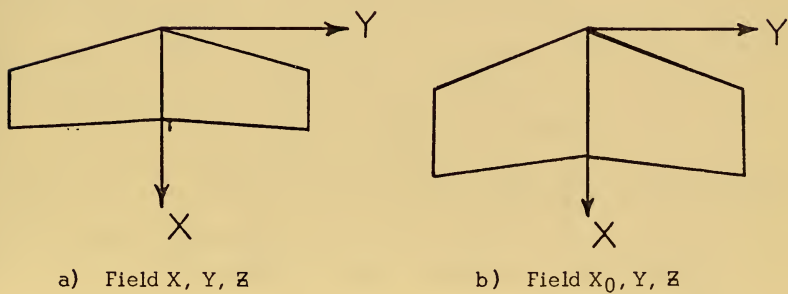


Figure 4. The effects of planform distortion.



From the total vortex strength at a chordal station, the section lift loadings can be obtained, i.e.,  $\Gamma_n = \sum_{i=1}^{Nc} \Delta \Gamma_i$  ---- (.10) and by application of the Kutta-Joukowski law,

$$\left(\frac{l}{q}\right)_n = 2 \frac{\Gamma_n}{V} \quad (.11)$$

The section moment may be obtained by taking the moments about a reference station of the individual bound vortex elements, inasmuch as the bound vortex elements represent the local air loading of each box by the Kutta-Joukowski law.

A two-dimensional study was made to compare the "pressure distribution" imposed by the vortices and the cotangent type pressure distribution as prescribed in theory (Ref. 2).

Assuming that the chordwise vortex elements described a chordwise pressure distribution, it appeared feasible to use a chordwise collocation technique for obtaining section lift coefficients and moment coefficients,  $C_l$  &  $C_{m_{c/4}}$ , given by

$$C_l = 2\pi A_0 + \pi A_1, \quad \& \quad C_{m_{c/4}} = \frac{\pi}{4} (A_2 - A_1)$$

Since  $\frac{\Delta p}{q} = \frac{2x}{V} \quad ; \quad \frac{x}{c} = \frac{1}{2} (1 - \cos \theta)$

and  $\frac{2x}{V} = 4 A_0 \cot \frac{\theta}{2} + 4 \sum_{n=1}^{\infty} A_n \sin n\theta$

it appeared that a solution for the Fourier coefficients could be found in the following relationship:

$$\left\{ \frac{\Delta p}{q} \right\} = 4 \begin{bmatrix} \cot \theta_{1/2} & \sin \theta_1 & \sin 2\theta_1 & \dots & \sin(n-1)\theta_1 \\ \vdots & \vdots & \vdots & \ddots & \vdots \\ \cot \theta_{n/2} & \sin \theta_n & \sin 2\theta_n & \dots & \sin(n-1)\theta_n \end{bmatrix} \{A_n\}$$





However, the existence of the  $A_n$ 's assumes knowledge of the pressure distribution over the wing, and correct results were not obtained, since the vortex strengths did not represent pressure loadings.

A check was made using two-dimensional theory to bear out these conclusions, and it was found that even for ten chordwise stations, the pressure distribution was incorrect, and the aerodynamic center was not located at the one-quarter chord. The leading edge singularity was not properly represented and the first collocation point differed from theory significantly. This check can be seen in Appendix D.

In light of these results, a straight-forward summation was used to obtain the section lift coefficients, i.e.,

$$C_l c = \sum_{i=1}^{NC} \left( \frac{\Delta \Gamma}{q} \right)_i \quad \text{---} \quad (.12)$$

## C. COMPRESSIBILITY CORRECTIONS FOR SUBSONIC FLOW

The compressibility corrections were obtained by the Prandtl-Glauert planform distortion method (Ref. 2). The applicable flow field equation for the velocity potential was given by

$$(1 - M_\infty^2) \phi_{xx} + \phi_{yy} + \phi_{zz} = 0 \quad \text{---} \quad (.13)$$

where the subscript represents second partial derivative. By use of the Prandtl-Glauert transformation,  $x = x_o \sqrt{1 - M_\infty^2}$  --- (.14)

this reduced equation (.13) to:

$$\phi_{x_o x_o} + \phi_{yy} + \phi_{zz} = 0 \quad \text{---} \quad (.15)$$



The effect of the Prandtl-Glauert transformation was to stretch all of the x-coordinates by the factor  $\frac{1}{\sqrt{1-M_\infty^2}}$ . The effects can be seen in Fig. 4.

The net effects of the planform distortion were as follows:

1) the aspect ratio was decreased; 2) the leading edge sweep was increased; 3) the taper ratio ( $C_t/C_r$ ) was unchanged; and 4) most importantly, the downwash distribution  $\left\{\frac{\omega}{V}\right\}$  was unchanged, i.e.,

$$\omega = \frac{\partial \phi}{\partial z} = \frac{\partial \phi}{\partial z_0} ; \quad z = z_0 \quad \text{---} \quad (1.16)$$

Since the downwash angle distribution,  $\left\{\frac{\omega}{V}\right\}$ , is unchanged in going from the distorted wing to the original wing, the aerodynamic loading distribution,  $\left\{\frac{\Delta l}{q}\right\}$ , will be the same on both wings. This is an important concept in that the aerodynamic loading obtained from the distorted planform under incompressible flow will be the same as the aerodynamic loading on the original planform under compressible flow. Hence the aerodynamic loading is an invariant when going from the compressible undistorted planform to the incompressible distorted planform.

#### D. STRUCTURAL ASPECTS OF THE PROBLEM

Because wings are flexible or elastic, there are always changes in angle of attack due to the deflections of the structure. There are two deflection modes present, torsion and bending, both affecting the changes in angle of attack distribution on the wing. The effects of these two modes were called static aero-elastic effects and have been



incorporated into the program by the simple elastic-axis beam representation.

The final angle of attack distribution  $\{\alpha_f\}$  was made up of two components  $\{\alpha_s\}$ , and  $\{\alpha_r\}$ , i.e.

$$\{\alpha_f\} = \{\alpha_s\} + \{\alpha_r\} \quad \text{---} \quad (.17)$$

Now the  $\{\alpha_s\}$  as shown in Ref. 1, has been determined to be:

$$\{\alpha_s\} = q[S]\left\{\frac{\Delta l}{q}\right\} \quad \text{---} \quad (.02)$$

See Appendix C for the development of the structural influence coefficient matrix  $[S]$ .

#### E. TOTAL SOLUTION TO THE PROBLEM

By combining equations .12, .17, and .02, the following relationship was formed:

$$[A]\left\{\frac{\Delta l}{q}\right\} = q[S]\left\{\frac{\Delta l}{q}\right\} + \{\alpha_r\}$$

$$\text{or } [A] - q[S]\left\{\frac{\Delta l}{q}\right\} = \{\alpha_r\} \quad \text{---} \quad (.18)$$

The closed form solution for aerodynamic loading distribution may be given as:

$$\left\{\frac{\Delta l}{q}\right\} = [A] - q[S]^{-1} \{\alpha_r\} \quad \text{---} \quad (.03b)$$

This was the final equation used in the program to obtain a chordwise and a spanwise loading distribution for a given surface.



## F. CALCULATION OF STABILITY DERIVATIVES

Five stability derivatives were investigated to check the validity of the program. These were:

$$C_{L_\alpha}, C_{m_\alpha}, C_{m_{c_L}}, C_{l_P}, \text{ \& } C_{l_{\delta a}}$$

The total wing  $C_L$  was obtained by a spanwise collocation technique, using the section lift coefficients.

$$\frac{L}{q b} = C_L C_{AVE} = \frac{1}{2} \int_{-1}^{+1} \left( \frac{l}{q} \right) d\eta \quad \text{---} \quad (19)$$

where  $\eta = \left( \frac{2y}{b} \right) = \cos \theta$  ;  $d\eta = -\sin \theta d\theta$

Let  $\frac{l}{q} = \frac{2\Gamma}{V} = \sum_{n=1}^{\infty} B_n \sin n\theta$

Then 
$$C_L C_{AVE} = \frac{1}{2} \int_0^\pi \sum_{n=1}^{\infty} B_n \sin n\theta \sin \theta d\theta$$
  

$$" = \frac{1}{2} \sum_{n=1}^{\infty} B_n \int_0^\pi \sin n\theta \sin \theta d\theta = \frac{\pi}{4} B_1$$

Since by orthogonality

$$\int_0^\pi \sin n\theta \sin \theta d\theta = \begin{cases} \frac{\pi}{2} & \text{FOR } n=1 \\ 0 & " \quad n \neq 1 \end{cases}$$

Therefore

$$C_L = \frac{\pi}{4} \frac{B_1}{C_{AVE}} \quad \text{---} \quad (20)$$

Since the assumption of linearized wing theory was made,

$$C_{L_\alpha} = \Delta C_L \text{ due to } \{\alpha_r\} \text{ input of 1.0 rad. uniformly over the whole wing, i.e. } C_{L_\alpha} = \frac{\Delta C_L}{\{\alpha_r = 1.0\}}$$

The  $C_{m_\alpha}$ 's were obtained by a straight-forward integration technique. In effect, the section pitching moment at the quarter chord was found to be:

$$\left( \frac{m}{q} \right)_n = C_{m_{c/4}} C_n^2 = \sum_{i=1}^{N_C} \left( \frac{\Delta l}{q} \right)_i (X_i - X_{c/4})$$





Hence, total wing pitching moment is:

$$C_{m_{\bar{c}/4}} = \frac{(4h)}{5\bar{c}} \left[ \frac{\Delta l}{q} \right] \{ (x - x_{\bar{c}/4}) \} \quad \text{---} \quad (.21)$$

Again  $C_{m_\alpha}$  was evaluated by:  $C_{m_\alpha} = \Delta C_m$

where  $\Delta C_m$  is pitching moment change about the wing  $\bar{c}/4$  point due to  $\{\alpha_r\} = 1.0$  rad. input.

With  $C_{L_\alpha}$  and  $C_{m_\alpha}$  calculated, the  $C_{m_{c_L}}$  was easily found by the following relationship:

$$C_{m_{c_L}} = \frac{dC_m}{dC_L} = \frac{C_{m_\alpha}}{C_{L_\alpha}} \quad \text{---} \quad (.22)$$

From the anti-symmetric solution of the Aero Matrix (see Appendix B), certain rolling moment derivatives were extracted. The rolling moment coefficients were obtained by a collocation technique, similar to that used to obtain the total wing  $C_L$ .

$$\begin{aligned} \frac{RM}{q b^2} &= C_l c_{AVE} = -\frac{1}{4} \int_{-1}^{+1} \left( \frac{z}{q} \right) \eta d\eta \\ " &= -\frac{1}{4} \int_0^\pi \sum_{n=1}^\infty B_n \sin n\theta \cos\theta \sin\theta d\theta \\ " &= -\frac{1}{8} \sum_{n=1}^\infty B_n \int_0^\pi \sin n\theta \sin 2\theta d\theta = -\frac{\pi}{16} B_2 \end{aligned}$$

where  $\int_0^\pi \sin n\theta \sin 2\theta d\theta = \begin{cases} \pi/2 & \text{for } n=2 \\ 0 & \text{" } n \neq 2 \end{cases}$

Therefore  $C_l = -\frac{\pi}{16} \frac{B_2}{C_{AVE}} \quad \text{---} \quad (.23)$



The roll damping derivative,  $C_{l_P}$ , was then obtained by placing the anti-symmetric angle of attack input on the wing, as shown in Figure 5. At the tip, the angle of attack =  $\frac{pb}{2V} = 1$  rad., and  $C_{l_P}$  was given by:

$$C_{l_P} = \frac{\partial C_l}{\partial (\frac{pb}{2V})} = \frac{\Delta C_l}{\{\alpha_r = \eta\}} \quad \text{---} \quad (.24)$$

The aileron control effectiveness,  $C_{l_{\delta_a}}$ , was found by defining the location of two of the boxes to coincide with the location of a typical set of ailerons, see Fig. 6. By inputting zero angle of attack everywhere on the wing except at the aileron locations and giving them 1.0 rad. angle of attack each, positive on one side of the wing and negative on the other, a rolling moment was produced.  $C_{l_{\delta_a}}$  was given by:

$$C_{l_{\delta_a}} = \frac{\partial C_l}{\partial \delta_a} = \frac{\Delta C_l}{\{\alpha_r \text{ DUE TO } \delta_a\}} \quad \text{---} \quad (.25)$$



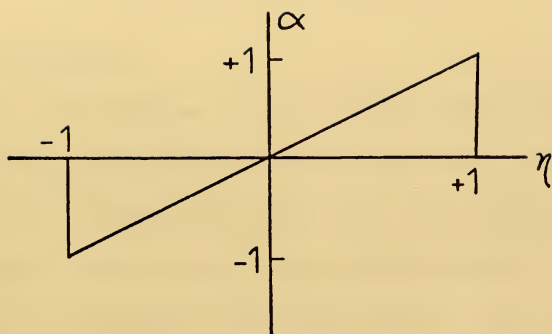


Figure 5. Angle of attack distribution for a constant rolling velocity  $P$ .

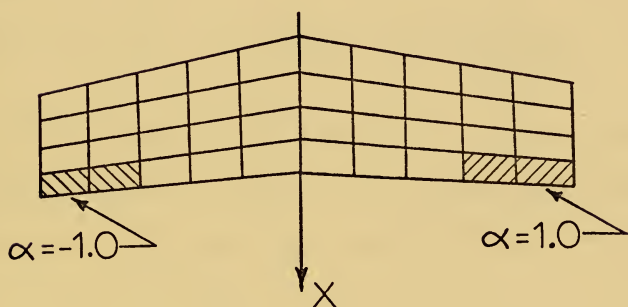


Figure 6. Ailerons as defined by horseshoe vortices.



### III. RESULTS AND DISCUSSION

#### A. LONGITUDINAL

The results from the symmetric portion of the program were checked by using longitudinal stability derivatives (i.e. lift-curve slope  $C_{L_\alpha}$ , moment-curve slope  $C_{m_\alpha}$ , and  $\frac{dC_m}{dC_L}$ ). To insure that changes in leading edge sweep and Mach number are handled correctly in the program, checks were made on  $C_{L_\alpha}$  and  $C_{m_\alpha}$ . These checks were made for a rigid wing with an aspect ratio of 6.0 and a taper ratio of 0.3.

Figure 7 shows the effects of leading edge sweep on lift-curve slope  $C_{L_\alpha}$ , and moment-curve slope  $C_{m_\alpha}$ . These curves were obtained by inputting a "do loop" in the program and varying the leading edge sweep  $\Lambda_{LE}$  from 0 to 40 degrees. These results agreed quite well with theory, i.e.  $(C_{L_\alpha})_\Lambda \approx \frac{(C_{L_\alpha})_{\Lambda=0}}{\sqrt{1 - M_\infty^2 \cos^2 \Lambda_{c/4}}} \dots (26)$

where the Mach number is held constant and the sweep varied.

Figure 8 shows the effects of the compressibility corrections in the program on  $C_{L_\alpha}$  and  $C_{m_\alpha}$ . Again a "do loop" was used, stepping through the program for Mach numbers of 0.0 to 0.9. These results also agreed with theory, i.e. equation (26), where the sweep is held constant and the Mach number varied.





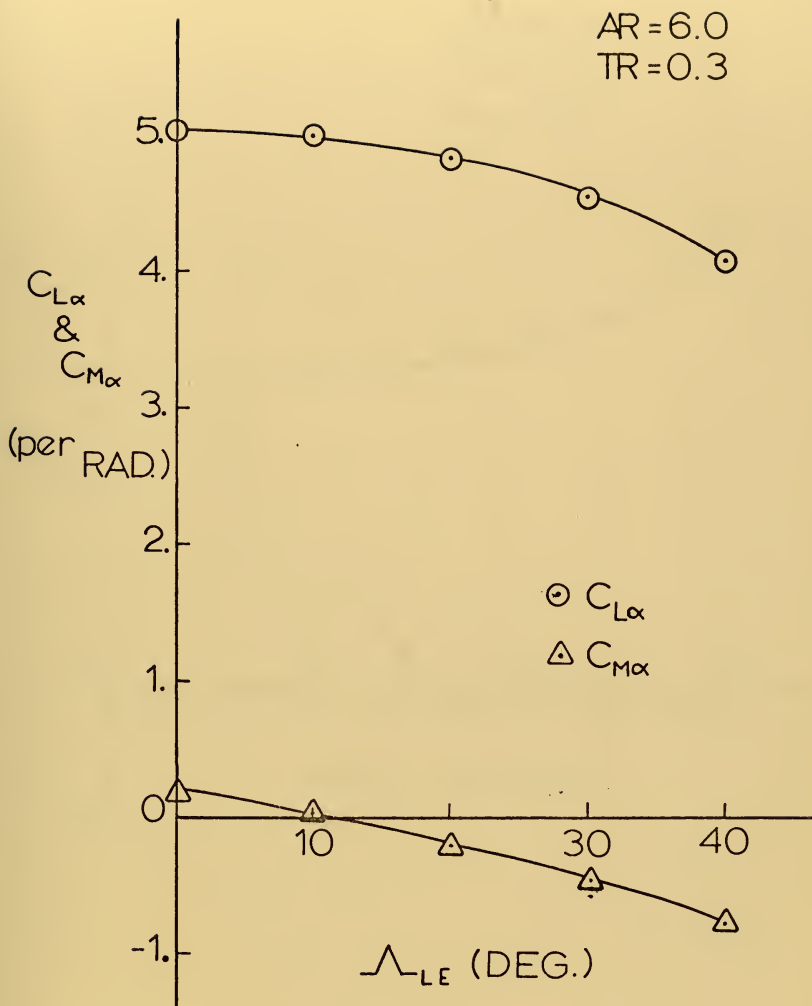


Figure 7. Lift-curve slope plotted as a function of leading edge sweep at a Mach number of 0.5.



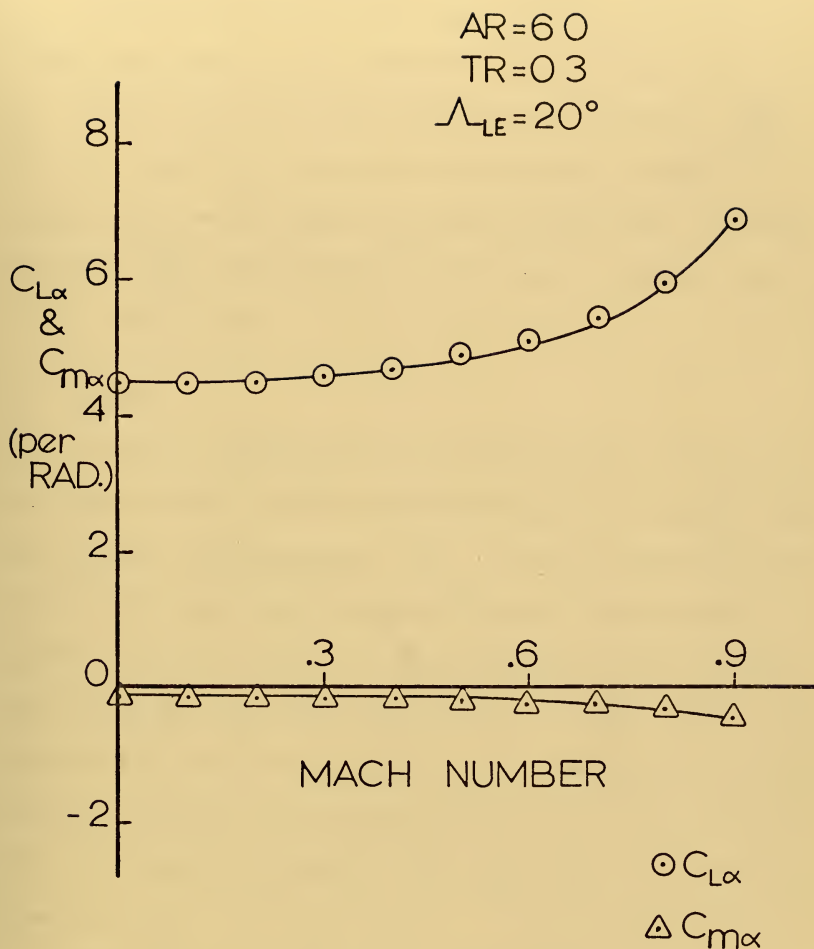


Figure 8. Lift-curve slope and moment-curve slope plotted as a function of Mach number with a leading edge sweep of 20.0 deg.



It should be noted that the  $C_{m\alpha}$  variation, with increasing leading edge sweep, is in a direction to shift the aerodynamic center aft. Figure 9 shows this more clearly since the value of  $\frac{dC_m}{dC_L}$  about the wing  $\bar{c}/4$  corresponds to the distance, in wing m.a.c. lengths, that the aero center is from the reference axis. A positive value of  $\frac{dC_m}{dC_L}$  indicates that the aero center is forward of the  $\bar{c}/4$  reference point.

## B. LATERAL

In order to document the anti-symmetric portion of the program, two lateral stability derivatives were investigated, roll damping  $C_{l_P}$  and roll due to aileron deflection  $C_{l_{\delta a}}$ . The aeroelastic effects were checked at the same time by choosing an example from Bisplinghoff, Ashley, and Halfman, Ref. 3. A typical jet transport with a straight taper and straight elastic axis defined at 35% c is used. The  $R$  for the wing was 6.15 and the taper ratio was 0.444. The bending and torsional stiffness properties of the wing were taken from Ref. 3, Fig. 2-29; then they were scaled to our model by  $(EI)_m = \frac{1}{\lambda^4} (EI)_P$  and reproduced here in Fig. 12.

The checks were made at a constant Mach number while varying the dynamic pressure ( $q$  in p.s.i.) from 0.0 (rigid wing) to 18.0, corresponding to varying the altitude. The effect of aeroelasticity upon roll damping for this wing, with an unswept quarter chord, is to increase the damping with an increase in  $q$ . Note that the sign on roll damping is negative since the moment that is developed is opposite to the direction



AR=6.0  
TR=0.3  
M=0.5

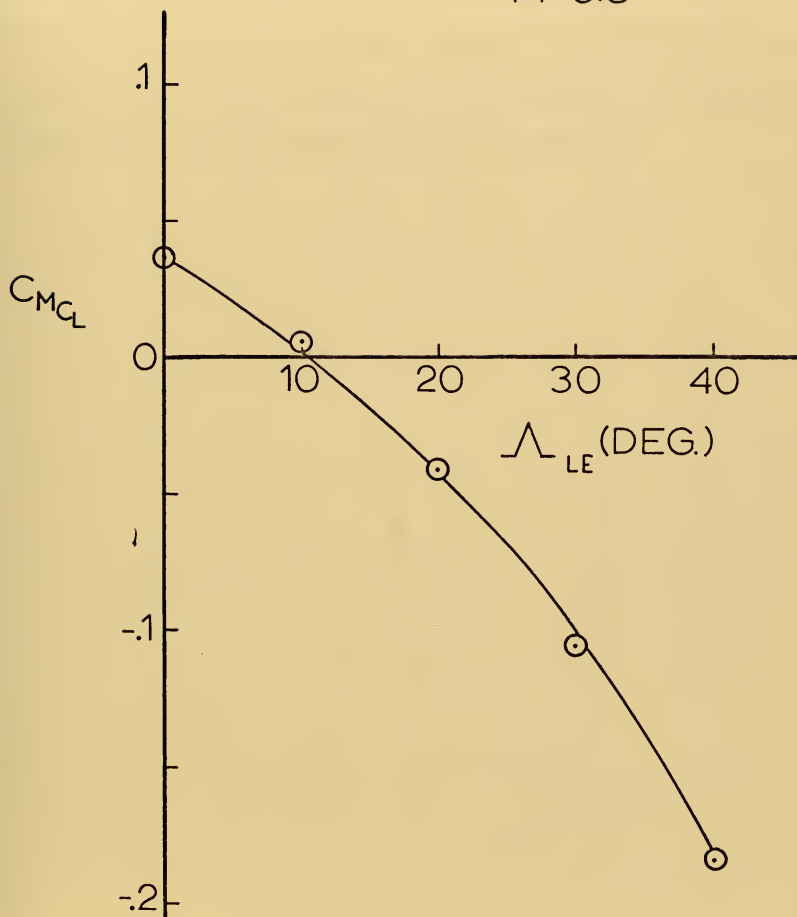


Figure 9. Static margin indicator plotted as a function of leading edge sweep at a Mach number of 0.5.





of roll. Figure 11 shows the roll damping derivative plotted as a function of  $q$ . The results of aeroelasticity upon the rolling moment due to aileron deflection can be seen in Fig. 10. Note that the change in sign corresponds to the control reversal dynamic pressure,  $q_r$ . The  $q_r$  was found to be 11.8 p.s.i., while it was shown to be 11.39 p.s.i. in Ref. 3, by another method; this is a difference of approximately 4%.



AR=6.154  
TR=0.444  
M=0.50

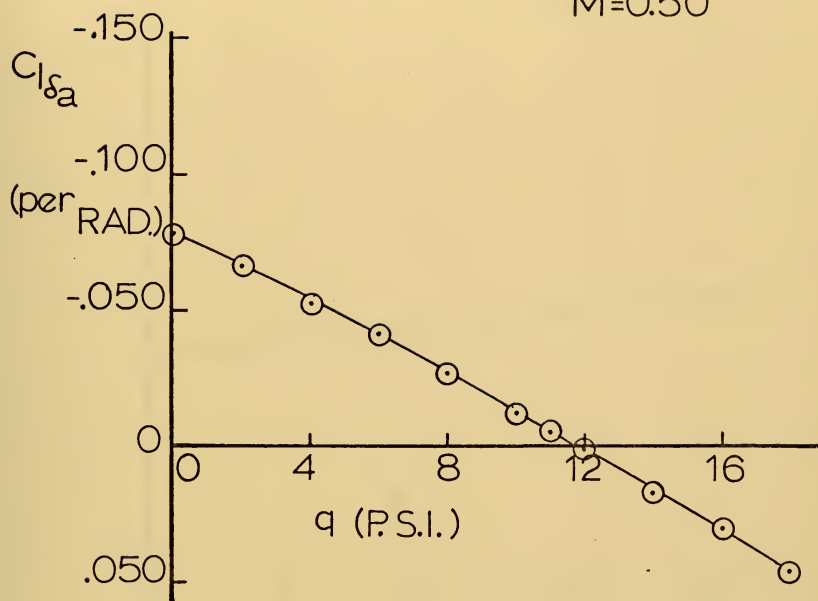


Figure 10. Rolling moment due to aileron deflection plotted as a function of free stream dynamic pressure at a Mach number of 0.5.



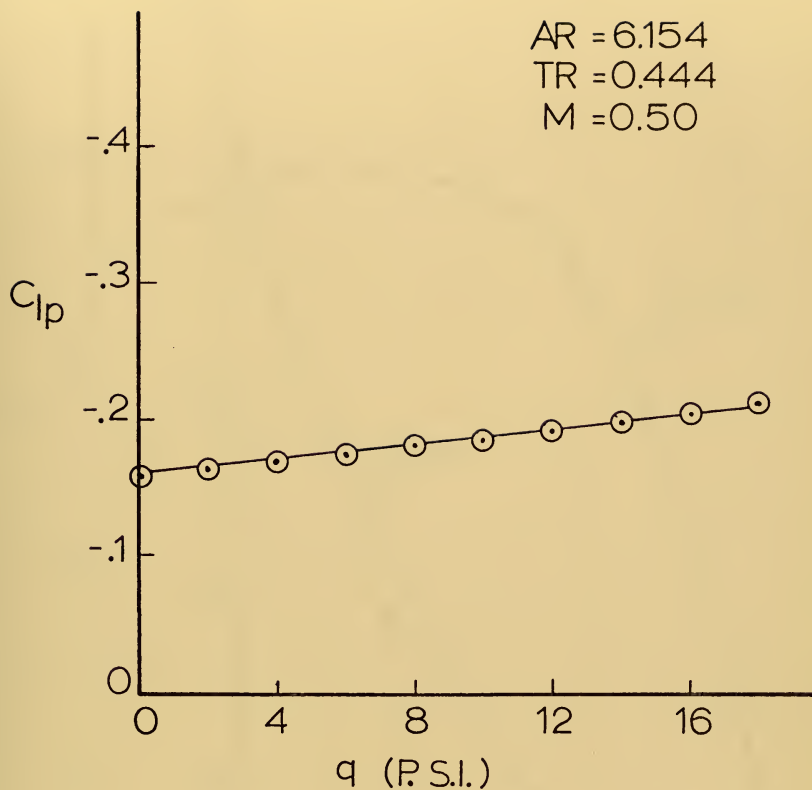


Figure 11. Damping in roll derivative plotted as a function of free stream dynamic pressure at a Mach number of 0.5.



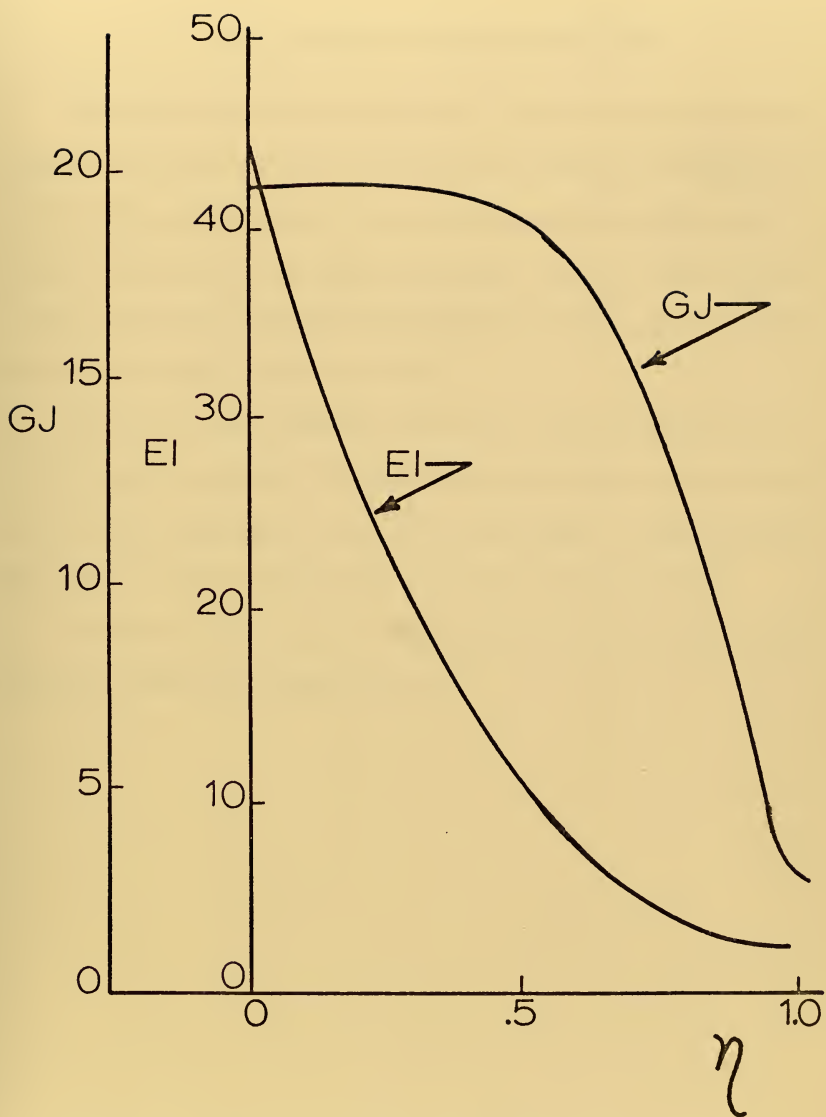


Figure 12. Bending and torsion stiffness curves.





#### IV. CONCLUSIONS AND RECOMMENDATIONS

This computer program can provide a 'limited' capability to make stability and control analyses of modern Navy aircraft. The program, as it now stands, is limited both to wings structurally compatible to the elastic-axis concept and to simple planforms. However, slight modifications could easily handle arbitrarily shaped wings and even a variable sweep configuration, such as the F-14.

The study is not complete at this point; a logical addition to the program would be to add the influence of the body radius to the Aero subroutine. This would improve the value of the program. If felt warranted, plate theory could be used for part or all of the structures matrix.

A follow-on study now seems appropriate to make the program more attractive and useful to design groups.



## APPENDIX A. ASSUMPTIONS

In writing this program, many theories with basic underlying assumptions were used. Most of them are associated with thin airfoil theory, or the structure of the wing. These assumptions, most of them listed by Gray and Schenk in Ref. 1, are as follows:

1. Potential flow about the wing with no boundary layer effects, i.e. inviscid, and without compression shocks, i.e. below transonic mach numbers.
2. The thickness ratio of the wing is small.
3. The lift-curve-slope,  $a_0 = 2\pi$ , i.e., two-dimensional
4. Changes in camber due to bending and torsion of the wing are neglected.
5. The changes in angle of attack due to structural deformations are uniform along each spanwise station.
6. The elastic deformation of the control surfaces is the same as that of the adjoining wing.
7. The angles of structural deformation are small such that
$$\sin \theta \cong \tan \theta \cong \theta \quad ; \quad \cos \theta \cong 1.0$$
8. Drag-load effects to deformation of the wing were neglected.



## APPENDIX B. DERIVATION OF THE AERO SUBROUTINE

The basic development of the downwash matrix or aerodynamic influence matrix was done by Gray and Schenk in Ref. 1. An expansion was made here to include swept-bound vortices and a chordwise, as well as spanwise, distribution of horseshoe vortices.

The lift or aero loading distribution over an airfoil can be characterized by a system of horseshoe vortices, each of these vortices contributing to the upwash or downwash at points all over the wing. Figure B1 shows two horseshoe vortices combined to make a wing. Conventional right hand rule indicates the sense of circulation associated with each horseshoe vortex. Quite obviously, the more horseshoe vortices used to approximate a wing, the more accurate the lift distribution obtained.

With the wing divided up into  $NC \times NS$  stations, the horseshoe vortices were placed at each quarter chord of the box, and the horseshoe vortex lattice, as shown in Fig. 1, was arrived at. Now the boundary conditions or flow tangency requirements, for simplicity of calculations, were imposed at the three-quarter chord<sup>1</sup> for each station or box. The boundary condition implies that the downwash angle  $\left(\frac{\omega}{V}\right)$  at each control station is equal to the geometric angle of attack. The downwash velocity  $\omega$  at each station is due to the sum of the downwash velocities induced by each horseshoe vortex over the entire wing.

---

<sup>1</sup>The chord for each box is equal to the local wing chord divided by  $NC$ .



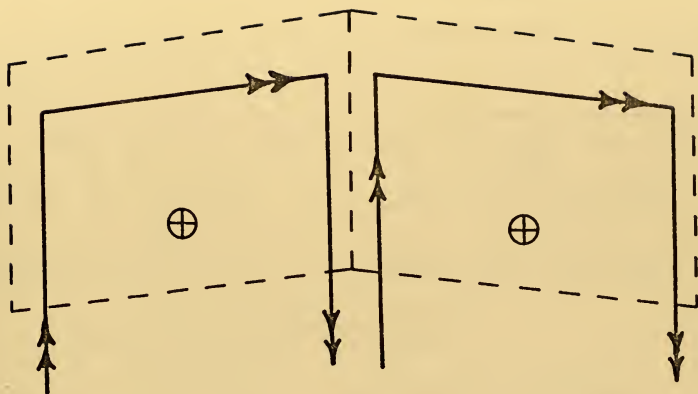


Figure B1. Simplified horseshoe vortices system for wing lift distribution.

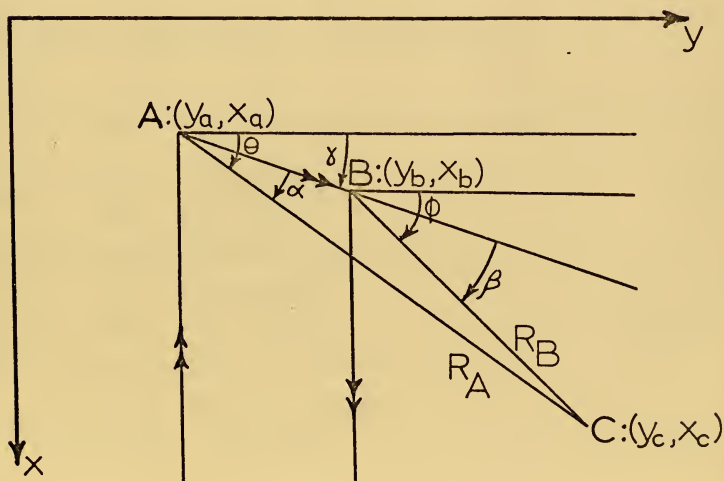


Figure B2. Geometry for downwash velocity calculation.





Given one horseshoe vortex and one control point on the same wing, as shown in Fig. B2, the downwash velocity  $\Delta w$  was calculated as follows:

$$\begin{aligned}
 R_A &= \sqrt{(y_c - y_A)^2 + (x_c - x_A)^2} \quad ; \quad R_B = \sqrt{(y_c - y_B)^2 + (x_c - x_B)^2} \\
 \sin \theta &= (x_c - x_A)/R_A \quad \sin \phi = (x_c - x_B)/R_B \\
 \cos \theta &= (y_c - y_A)/R_A \quad \cos \phi = (y_c - y_B)/R_B \\
 l_{AB} &= \sqrt{(y_B - y_A)^2 + (x_B - x_A)^2} \\
 \sin \gamma &= (x_B - x_A)/l_{AB} \quad \cos \gamma = (y_B - y_A)/l_{AB} \\
 \alpha &= \theta - \gamma \quad \beta = \phi - \gamma \\
 \sin \alpha &= \sin \theta \cos \gamma - \cos \theta \sin \gamma \\
 \cos \alpha &= \cos \theta \cos \gamma + \sin \theta \sin \gamma \\
 \cos \beta &= \cos \phi \cos \gamma + \sin \phi \sin \gamma
 \end{aligned}$$

The left hand vortex contribution to the downwash velocity was given by:

$$\Delta w_L = \frac{\Gamma}{4\pi} \frac{(1 + \sin \theta)}{(y_c - y_A)} \quad \text{----} \quad (\text{B.01})$$

The right hand vortex contribution was given by:

$$\Delta w_R = \frac{-\Gamma}{4\pi} \frac{(1 + \sin \phi)}{(y_c - y_B)} \quad \text{----} \quad (\text{B.02})$$

The bound vortex contribution was given by:

$$\Delta w_B = \frac{\Gamma}{4\pi} \frac{(\cos \alpha - \cos \beta)}{R_A \sin \alpha} \quad \text{----} \quad (\text{B.03})$$



If the control point happened to be on a straight line extension of the bound vortex, both numerator and denominator would go to zero simultaneously. The contribution from the bound vortex would be zero and a check was placed into the program and if this situation were to develop,  $\Delta\omega_B$  would be set to zero.

The total contribution to the downwash velocity due to the one horseshoe vortex on the same wing was:

$$\Delta\omega = \Delta\omega_C + \Delta\omega_L + \Delta\omega_B$$

$$\text{or } \Delta\omega = \frac{\Gamma}{4\pi} \left[ \frac{(1 + \sin\Theta)}{(y_C - y_A)} - \frac{(1 + \sin\Phi)}{(y_C - y_B)} + \frac{(\cos\alpha - \cos\beta)}{R_A \sin\alpha} \right] \quad (\text{B.04})$$

The downwash velocity contribution at control points all over the wing, due to a horseshoe vortex system, was calculated in a similar manner. These can be thought of in matrix format as follows:

$$\begin{Bmatrix} \omega_1 \\ \omega_2 \\ \vdots \\ \omega_N \end{Bmatrix} = \begin{Bmatrix} \Delta\omega_{11} + \Delta\omega_{12} + \dots + \Delta\omega_{1N} \\ \Delta\omega_{21} + \Delta\omega_{22} + \dots + \Delta\omega_{2N} \\ \vdots \\ \Delta\omega_{N1} + \Delta\omega_{N2} + \dots + \Delta\omega_{NN} \end{Bmatrix}$$

where the subscripts indicate the downwash at station  $i$  due to a horseshoe vortex at station  $j$ , etc. Now by factoring a  $\Gamma$  from each term in the proper manner:

$$\{\omega\} = 2[A]\{\Gamma\}$$

then the following relationship follows:



$$\left\{ \frac{w}{V} \right\} = [A] \left\{ \frac{2\Gamma}{V} \right\} \quad \text{---} \quad (\text{B.05})$$

$$\text{or} \quad \left\{ \frac{w}{V} \right\} = [A] \left\{ \frac{\Delta l}{q} \right\} \quad \text{---} \quad (\text{B.06})$$

$$\text{Now} \quad \left\{ \frac{w}{V} \right\} = \{ \alpha_f \} ; \therefore \{ \alpha_f \} = [A] \left\{ \frac{\Delta l}{q} \right\} \quad \text{---} \quad (\text{B.07})$$

The A matrix is the aero-influence matrix as used in the program.

The computations are carried out for contributions from each wing, i.e.

$$[A_R] \text{ \& } [A_L]$$

$$\text{For symmetric loads:} \quad \left. \begin{aligned} [AS] &= [A_R] + [A_L] \end{aligned} \right\} \quad (\text{B.03a,b})$$

$$\text{For anti-symmetric loads:} \quad [AA] = [A_R] - [A_L]$$

$$\text{Then} \quad \left\{ \alpha_f \right\} = [AS \text{ or } AA] \left\{ \frac{\Delta l}{q} \right\}_{\text{R.H. SIDE}}$$

Also contained in the Aero subroutine is the Prandtl-Glauert planform distortion correction for subsonic compressibility. In essence, all of the x distances are stretched by a factor of  $(1 - M_\infty^2)^{-1/2}$ , defined as  $\beta$ . Therefore throughout the subroutine  $f(\beta x, y)$  replaces  $f(x, y)$ . (i.e.  $\beta(x_c - x_A)$  instead of  $(x_c - x_A)$  ).

The 'lifting-surface' representation of a wing has been written up in FORTRAN IV for use with the IBM 360-67 computer. The program was designed to handle planforms of low to high aspect ratio, swept leading edges, and a linear taper ratio. The choice of the number of stations on the wing, chordwise and spanwise, was left arbitrary for easy compatibility with most wings and for almost any flap and aileron arrangement.



So as to make the program more flexible, subroutines were used for each phase of the calculations. Subroutine Geom is used for locating the horseshoe vortices and their control points; subroutine Aero is used for obtaining the aerodynamic influence (or downwash) matrix; and subroutine Struct is used for obtaining the structural influence coefficient matrix. With the subroutine packages set up as they were, changes to the program can be easily handled simply by making small changes in the input or the main program.

Sample calculations were made for arbitrary wing geometries. The results of these calculations can be seen in the main text.

The desired results were obtained in these calculations. The corrections for subsonic compressibility, sweepback, and static aero-elastic effects have been checked and do give the desired accuracy.





## APPENDIX C. DERIVATION OF STRUCTURES SUBROUTINE

As in Appendix B, the  $[S]$ , structures matrix or elasticity matrix, was developed by Gray and Schenk in Ref. 1. An expansion to fit 'lifting-surface' theory vice 'lifting-line' theory was made for this program.

The problem was basically stated as: Given a loading over a wing, find the deformation imparted to the wing and apparent change in angle of attack. From the previous subroutine,

$$\{\alpha_f\} = [A] \left\{ \frac{\Delta l}{q} \right\} \quad \text{--- --} \quad (B.07)$$

The following relationship was obtained from this subroutine:

$$\{\alpha_s\} = q [S] \left\{ \frac{\Delta l}{q} \right\} \quad \text{--- --} \quad (.02)$$

The assumption has been made that the wing acts like a beam with the elastic axis representation. (See Refs. 1 and 4.) The beam bending and torsional moments have been resolved about the elastic axis at each spanwise station of the wing. Although the elastic axis may be arbitrary, it was thought of as a straight line for simplification here (see Fig. C1).

The wing is divided evenly in the spanwise direction with each of the chordal strips having width  $2h$ . Therefore for the wing with an assumed unit value of semispan,  $h = 1/2 (NS)$  --- -- (C.01)  
Positive direction for torsion and bending moments are shown in Fig. C1 relative to the elastic axis orientation.



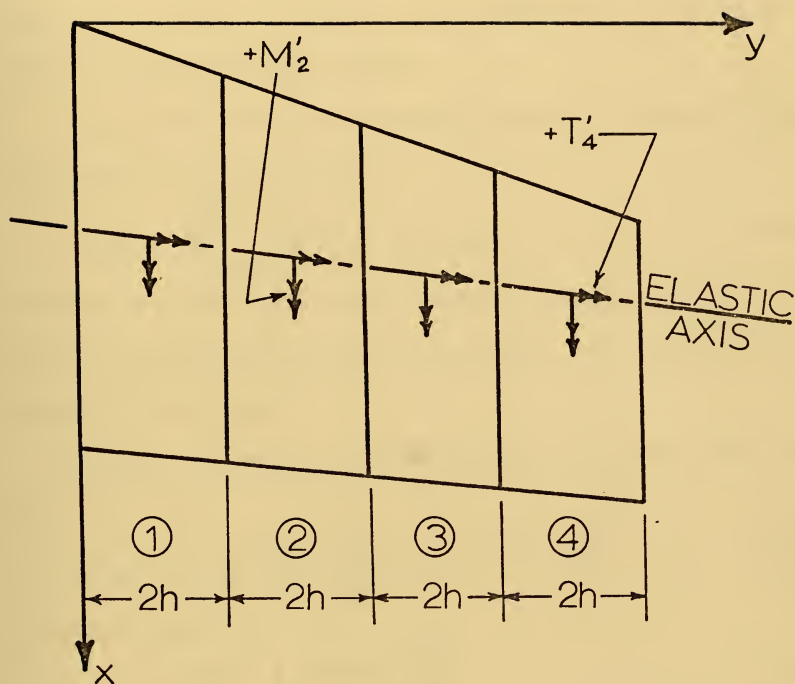


Figure C1. Elastic axis representation of the wing with the torques and moments at the station elastic axis points.



The span loads per unit span length are defined as  $\frac{\Delta l}{q}$  for the N vortex lattice boxes in a numbering sequence starting from N = 1 at the most forward, inboard box proceeding aft to the trailing edge at N = NC, then stepping to the next outboard set of boxes at the leading edge box for N = NC+1. Continue in this manner until the Nth box at the trailing edge of the tip is reached.

The individual lift force contribution towards the bending of the kth wing station may be expressed as:

$$\Delta L_i = \sum_{j=(iNC)+1}^{i(NC+1)} \left( \frac{\Delta l}{q} \right)_j (2 - \delta_{ik}) q h \quad \text{--- (C.02)}$$

The presence of the Kroecker delta takes into account that only one-half of the air loading at the kth station contributes to the bending (and torsion) moment at the kth station.

Therefore the bending moment at the kth station may be expressed as:

$$M_k = \Delta L_k \left( \frac{h}{2} \right) + \sum_{j=k+1}^{NS} \Delta L_j (2h)(j-k) \quad \text{--- (C.03)}$$

or in matrix notation as:

$$\{M\} = q [AM] \left\{ \frac{\Delta l}{q} \right\} \quad \text{--- (C.04)}$$

where

$$\{M\} = NS \times 1 \quad \text{column vector}$$

$$\left\{ \frac{\Delta l}{q} \right\} = N \times 1 \quad \text{column vector}$$

$$[AM] = NS \times N \quad \text{rectangular matrix, and}$$



$$[AM] = h^2 \begin{bmatrix} \frac{1}{2} & 4 & 8 & 12 & 16 & \cdots \\ 0 & \frac{1}{2} & 4 & 8 & 12 & \cdots \\ 0 & 0 & \frac{1}{2} & 4 & 8 & \cdots \\ 0 & 0 & 0 & \frac{1}{2} & 4 & \cdots \\ \vdots & \vdots & \vdots & \vdots & \frac{1}{2} & \cdots \\ \vdots & \vdots & \vdots & \vdots & \vdots & \ddots \end{bmatrix}$$

The AM matrix was partitioned into NS x NS elements where each element is a (1 x NC) row matrix made up of constants as indicated, i.e.

$$\begin{bmatrix} \frac{1}{2} \end{bmatrix} = \left[ \frac{1}{2} \quad \frac{1}{2} \quad \dots \quad \frac{1}{2} \right]$$

The torsion moment at the kth station may be expressed as:

$$T_k = q [AT] \left\{ \frac{\Delta l}{q} \right\} \quad (.05)$$

where

$$[AT] = h \begin{bmatrix} \Delta X_{11} \cdots \Delta X_{1,NC} & 2\Delta X_{1,NC+1} \cdots 2\Delta X_{1,2NC} \\ \cdots & \cdots \\ 0 & \Delta X_{2,NC+1} \cdots \Delta X_{2,2NC} \\ \cdots & \cdots \\ 0 & 0 \\ \vdots & \vdots \end{bmatrix}$$

and

$$\Delta X_{kj} = (X_{EA})_k - (X_{CA})_j$$

where

$$1 \leq k \leq NS \quad \& \quad 1 \leq j \leq N = NC \times NS$$

The zero partition elements to the left of the lead diagonal correspond to inboard loadings that do not contribute to the moments at stations outboard.





The torsional and bending moments as developed here were perpendicular and parallel respectively to the streamwise flow at the elastic axis reference points. In order to reorient them relative to the elastic axis, they were put through the following rotation matrix:

$$\begin{Bmatrix} M' \\ T' \end{Bmatrix} = \begin{bmatrix} \cos \Lambda_{EA} & -\sin \Lambda_{EA} \\ \sin \Lambda_{EA} & \cos \Lambda_{EA} \end{bmatrix} \begin{Bmatrix} M \\ T \end{Bmatrix} \quad \text{--- (C.06)}$$

Now the moment and torque distributions have been resolved to be the following relationships:

$$\begin{aligned} \begin{Bmatrix} M' \\ T' \end{Bmatrix} &= q \left[ \begin{bmatrix} \cos \Lambda_{EA} \\ \sin \Lambda_{EA} \end{bmatrix} [AM] - \begin{bmatrix} -\sin \Lambda_{EA} \\ \cos \Lambda_{EA} \end{bmatrix} [AT] \right] \begin{Bmatrix} \Delta l \\ q \end{Bmatrix} \\ \begin{Bmatrix} T' \end{Bmatrix} &= q \left[ \begin{bmatrix} \sin \Lambda_{EA} \\ \cos \Lambda_{EA} \end{bmatrix} [AM] + \begin{bmatrix} \cos \Lambda_{EA} \\ -\sin \Lambda_{EA} \end{bmatrix} [AT] \right] \begin{Bmatrix} \Delta l \\ q \end{Bmatrix} \quad \text{--- (C.07)} \end{aligned}$$

The change in angle of attack in the streamwise direction was obtained by the relationship (see Ref. 1):

$$\alpha_{s_n} = \int_0^{\eta} \frac{m M ds}{EI} + \int_0^{\eta} \frac{t T ds}{GJ} \quad \text{--- (C.08)}$$

where  $m$  equals the beam bending moment per unit pitching moment at the station  $\eta$ , and  $t$  equals the torsion about the elastic axis per unit pitching moment.  $ds \Rightarrow \frac{2h}{\cos \Lambda_{EA}} \quad \text{--- (C.09)}$

The above integral equation was changed to an algebraic equation by summing the contributions at each station.

$$\begin{aligned} \alpha_{s_1} &= \left( \frac{m_{11} M_1 h_1}{(EI)_1 \cos \Lambda_1} + \frac{2 m_{21} M_2 h_2}{(EI)_2 \cos \Lambda_2} + \dots \right) \\ &+ \left( \frac{t_{11} T_1 h_1}{(GJ)_1 \cos \Lambda_1} + \frac{2 t_{21} T_2 h_2}{(GJ)_2 \cos \Lambda_2} + \dots \right) \quad \text{(C.10)} \end{aligned}$$



The influence coefficients  $m_{ij}$  and  $t_{ij}$  were easily defined by the geometry of the problem and found to be as follows:

$$m_{ij} = \begin{cases} -\sin \Lambda_i & \text{where the point } i \text{ is outboard of the point } j \\ 0 & \text{where the point } i \text{ is at or inboard of the point } j \end{cases}$$

$$\text{and } t_{ij} = \begin{cases} \cos \Lambda_i & \text{for station } i \text{ outboard of station } j \\ 0 & \text{for station } i \text{ at or inboard of station } j \end{cases}$$

In matrix form the  $m_{ij}$ 's and  $t_{ij}$ 's were written as follows:

$$[m] = \begin{bmatrix} -\frac{\sin \Lambda_1}{2} & -\sin \Lambda_2 & -\sin \Lambda_3 & - & - & - \\ 0 & -\frac{\sin \Lambda_2}{2} & -\sin \Lambda_3 & - & - & - \\ 0 & 0 & -\frac{\sin \Lambda_3}{2} & - & - & - \\ \vdots & \vdots & \vdots & & & \end{bmatrix}$$

$$[t] = \begin{bmatrix} \frac{\cos \Lambda_1}{2} & \cos \Lambda_2 & \cos \Lambda_3 & - & - & - \\ 0 & \frac{\cos \Lambda_2}{2} & \cos \Lambda_3 & - & - & - \\ 0 & 0 & \frac{\cos \Lambda_3}{2} & - & - & - \\ \vdots & \vdots & \vdots & & & \end{bmatrix}$$

Now

$$\{\alpha_s\} = [m] \left[ \frac{2h}{EI \cos \Lambda} \right] \{M'\} + [t] \left[ \frac{2h}{GJ \cos \Lambda} \right] \{T'\} \quad (C.11)$$



Thus the desired form was achieved and the S matrix was:

$$[S] = \left[ [m] \left[ \frac{2h}{EI \cos \Lambda} \right] \left[ \cos \Lambda \right] [AM] - \left[ \sin \Lambda \right] [AT] \right] \\ + \left[ [t] \left[ \frac{2h}{GJ \cos \Lambda} \right] \left[ \sin \Lambda \right] [AM] + \left[ \cos \Lambda \right] [AT] \right] \quad \text{--- (C.12)}$$

The final resultant matrix equation was:

$$\{\alpha_s\} = q [S] \left\{ \frac{\Delta l}{q} \right\} \quad \text{--- (C.02)}$$

The computer program is normalized such that the wing semispan has unit length. However, an actual wing will have a finite wing span of say  $b/2$  inches, will operate at a dynamic pressure of  $q$  p.s.i., and will have stiffness properties of  $EI$  and  $GJ$  in units of  $\text{lb-in}^2$ .

Recognize that in a scaling analysis the structural twist of the model will equal the structural twist of the prototype and that they will operate at the same dynamic pressure. However, the aerodynamic loadings will differ by a factor of  $\lambda$

$$\text{where } \lambda = \frac{(b/2)_p}{(b/2)_m} = \left(\frac{b}{2}\right)_p \text{ since } \left(\frac{b}{2}\right)_m = 1 \quad \text{(C.13)}$$

$$\text{i.e. } \left\{ \frac{\Delta l}{q} \right\}_m = \frac{1}{\lambda} \left\{ \frac{\Delta l}{q} \right\}_p \quad \text{(C.14)}$$

Therefore by equation (C.02) we can scale

$$[S]_m = \lambda [S]_p$$

but analysis of equation (C.12) reveals that  $[S] \propto h^3/EI, h^3/GJ$

$$\text{so } \frac{[S]_m}{[S]_p} \propto \frac{[h^3/EI]_m}{[h^3/EI]_p}$$

$$\text{but } \left. \begin{aligned} \frac{h_m}{h_p} &= \frac{1}{\lambda} ; \therefore (EI)_p = \lambda^4 (EI)_m \\ (GJ)_p &= \lambda^4 (GJ)_m \end{aligned} \right\} \quad \text{--- (C.15)}$$



# APPENDIX D. TWO-DIMENSIONAL WING PRESSURE LOADING CONVERGENCE CHECK

In this appendix, a check was made to ascertain the validity of viewing the vortex strengths of the control boxes as pressure differentials. A comparison was made for the  $C_p$ 's obtained by this assumption, using a collocation technique for obtaining a chordwise pressure distribution, and the theoretical  $C_p$ 's with a cotangent type pressure distribution.

A two-dimensional section with unit chord was chosen for this check. The section was divided into N equal chordwise stations with the vortices placed at the quarter-chord of each station and the control points at the three-quarter chord of each station (see Fig. D1).

Since  $\Gamma_1, \Gamma_2, \dots, \Gamma_N$  represent the small vortex strengths concentrated at the quarter chord for each station, the total vortex strength was given by:

$$\begin{aligned} \text{Now } \Delta \lambda_i &= \rho V \Gamma_i & \frac{1}{\rho} \Delta P_i &= \frac{\Delta \lambda_i}{\Delta C} = \frac{\rho V \Gamma_i}{C/N} \\ \text{and } \Delta C_{P_i} &= \frac{\Delta P_i}{\frac{1}{2} \rho V^2} = \frac{2}{(1/N)} \left( \frac{\Gamma_i}{V} \right) \quad \text{--- --- ---} \quad (D.01) \end{aligned}$$

The principle of an infinite vortex (Ref. 2) was used for the downwash angles, i.e.  $\frac{\omega}{V} = \frac{1}{2\pi R} \left( \frac{\Gamma}{V} \right)$  or

$$\left\{ \frac{\omega}{V} \right\} = \frac{1}{2\pi} [B] \left\{ \frac{\Gamma}{V} \right\} \quad \text{--- --- ---} \quad (D.02)$$

where  $\frac{\omega}{V} = \alpha$  at the three-quarter chord control point, and

$$B_{ij} = \frac{1}{x_{c_i} - x_{A_j}} \quad \text{--- --- ---} \quad (D.03)$$





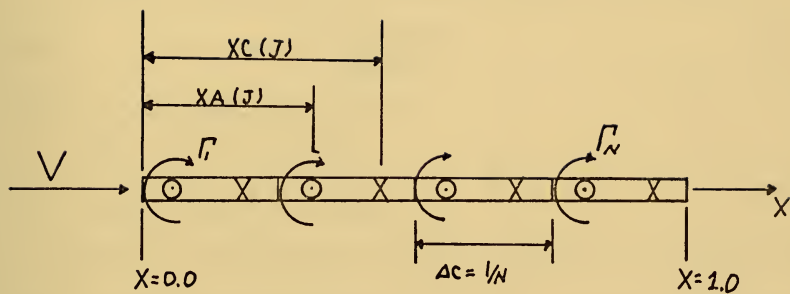


Figure D1. Geometry for two-dimensional study of chordwise pressure distribution.



with  $X_{A_j} = \frac{1}{N} j - \frac{0.75}{N}$  , the local quarter chord point,  
 and  $X_{C_i} = \frac{1}{N} i - \frac{0.25}{N}$  , the local three-quarter chord point.

$$\text{Hence } \{\Delta C_P\} = 4\pi N [B]^{-1} \{\alpha\} \quad \text{---} \quad (D.04)$$

with  $\alpha = 1.0$  radian for each station.

Now the theoretical  $\Delta C_p$  for two dimensions was given by

$$(\text{Ref. 2}): \quad \Delta C_P = 4 \frac{(1 + \cos \theta)}{\sin \theta} \quad \text{---} \quad (D.05)$$

using the coordinate transformation:

$$\left. \begin{aligned} \frac{x}{c} &= \frac{1}{2} (1 - \cos \theta) \\ \theta &= \cos^{-1} [1 - 2(\frac{x}{c})] \end{aligned} \right\} \quad \text{---} \quad (D.06)$$

Since the check was made at  $\alpha = 1.0$  radian and a unit chord, the  $C_{lc}$  obtained will be equivalent to  $C_{l\alpha}$  and should be approximately  $2\pi$  . The aerodynamic center given by:  $AC = \frac{C_{m_{LE}}}{C_{l\alpha}}$  (D.07) should be at 0.25c or just 0.25 in this case.

The tabulation in Fig. D2 clearly shows that the correct results were not obtained by the method as described herein.



| Station | Vortex Location | Theoretical |        | Section load | Theoretical<br>Section load | Aero Center | Theoretical<br>Aero Center |
|---------|-----------------|-------------|--------|--------------|-----------------------------|-------------|----------------------------|
|         |                 | CP          | CP     |              |                             |             |                            |
| 1       | 0.125           | 9.425       | 10.580 |              |                             |             |                            |
| 2       | 0.625           | 3.142       | 3.098  |              |                             |             |                            |
| 1       | 0.0625          | 13.740      | 15.490 | 5.7894       | 6.2832                      | 0.267       | 0.250                      |
| 2       | 0.3125          | 5.890       | 5.933  |              |                             |             |                            |
| 3       | 0.5625          | 3.534       | 3.528  | 5.8802       | 6.2832                      | 0.266       | 0.250                      |
| 4       | 0.8125          | 1.963       | 1.922  |              |                             |             |                            |
| 1       | 0.0417          | 17.01       | 19.18  |              |                             |             |                            |
| 2       | 0.2083          | 7.731       | 7.797  |              |                             |             |                            |
| 3       | 0.3750          | 5.154       | 5.164  |              |                             |             |                            |
| 4       | 0.5417          | 3.682       | 3.679  | 5.9338       | 6.2832                      | 0.264       | 0.250                      |
| 5       | 0.7083          | 2.577       | 2.567  |              |                             |             |                            |
| 6       | 0.8750          | 1.546       | 1.512  |              |                             |             |                            |
| 1       | 0.0313          | 19.74       | 22.27  |              |                             |             |                            |
| 2       | 0.1563          | 9.213       | 9.295  |              |                             |             |                            |
| 3       | 0.2813          | 6.378       | 6.394  |              |                             |             |                            |
| 4       | 0.4063          | 4.832       | 4.836  |              |                             |             |                            |
| 5       | 0.5313          | 3.750       | 3.757  | 5.9695       | 6.2832                      | 0.263       | 0.250                      |
| 6       | 0.6563          | 2.899       | 2.895  |              |                             |             |                            |
| 7       | 0.7813          | 2.126       | 2.117  |              |                             |             |                            |
| 8       | 0.9063          | 1.316       | 1.287  |              |                             |             |                            |
| 1       | 0.0250          | 22.14       | 24.98  |              |                             |             |                            |
| 2       | 0.1250          | 10.49       | 10.58  |              |                             |             |                            |
| 3       | 0.2250          | 7.403       | 7.424  |              |                             |             |                            |
| 4       | 0.3250          | 5.758       | 5.765  |              |                             |             |                            |
| 5       | 0.4250          | 4.651       | 4.653  |              |                             |             |                            |
| 6       | 0.5250          | 3.805       | 3.805  | 5.9953       | 6.2832                      | 0.262       | 0.250                      |
| 7       | 0.6250          | 3.101       | 3.098  |              |                             |             |                            |
| 8       | 0.7250          | 2.468       | 2.464  |              |                             |             |                            |
| 9       | 0.8250          | 1.851       | 1.842  |              |                             |             |                            |
| 10      | 0.9250          | 1.165       | 1.139  |              |                             |             |                            |

Figure D2. A tabulation of the two-dimensional wing convergence check.









```

SLE=0.0
DO 240 NN=1,5
  BMACH(1)=0.0
DO 240 N=1,10
  VI=BMACH(N)*1116.89
Q=0.0
BMACH1=BMACH(N)
CALL GEOM
CALL AERO
INPUT AN ANGLE OF ATTACK DISTRIBUTION OF ALPHA = 1.0 EVERYWHERE CORRESPONDING
TO A SYMMETRIC DISTRIBUTION.
DO 10 I=1,NZ
  ALPHA(I)=1.0
10 CONTINUE
DO 15 I=1,NZ
  DO 15 J=1,NZ
    U(I,J)=AS(I,J)-Q*S(I,J)
    ELU AND SLVB SOLVE THE EQUATION : (AS-Q*S)*(L/Q) = ALPHA
    CALL ELU(U,NZ,20)
    CALL SLVB(U,NZ,20,ALPHA)
  WRITE(6,20)
20 FORMAT('O',10X,'PROGRAM CHECK OF LOAD DISTRIBUTION:',//,15X,
1,ALPHA=1.0 RAD,/,3X,'STA',4X,'ETA',8X,'X',5X,'DEL(L/Q)',//)
  XC1=0.5*(XA(I)+XB(I))
  WRITE(6,21)I,YC(I),XC1,ALPHA(I)
21 FORMAT(2X,13,F10.6)
30 CONTINUE
X=NZ-NC+1
DO 40 I=1,NS
  THETA(I)=DARCOS(YC(K))
  NC1=(I-1)*NC+1
  NC2=I*NC
  IF(I.EQ.NS) GO TO 31
  K=K-NC
31 CLC(I)=0.0
  DO 40 J=NC1,NC2
    CLC(I)=CLC(I)+ALPHA(J)
40 CONTINUE
NOW A COLLOCATION TECHNIQUE IS SET UP TO INTEGRATE THE LIFT DISTRIBUTION TO
OBTAIN THE LIFT-CURVE SLOPE AND MOMENT-CURVE SLOPE. THE THETA'S ARE THE
COLLOCATION POINTS.
K=1
DO 41 I=NSP1,NS2
  THETA(I)=DARCOS(-YC(K))
  K=K+NC
41 CONTINUE

```



```

DO 70 I=1,NS
  CL(I)=CLC(I)/C(I)
CONTINUE
70  WRITE(6,111)
111  FORMAT(//,15X,'SECTION LEFT COEFFICIENTS',//,4X,'STA',5X,'CL',//)
112  FORMAT(15X,11,3X,F10.6)
      CAVE=2.0/AR
DO 200 I=1,NS2
  DO 200 J=1,NS2
    AJ=J
    R(I,J)=DSIN(AJ*THETA(I))
200  CONTINUE
    CN 201 I=1,NS
    CLC(I)=CLC(NSPI-I)
201  CONTINUE
    CO 202 I=NSPI,NS2
    CLC(I)=CLC(I-NS)
202  CONTINUE
NOW ELU AND SLVB ARE USED TO SOLVE FOR THE FOURIER COEFFICIENTS.
      CALL ELU(B,NS2,10)
      CALL SLVB(B,NS2,10,CLC1)
203  WRITE(6,203,11,3X,F10.6)
      CLT(N)=PI/4.0*CLC1(1)/CAVE
      CRM=PI/16.0*CLC1(2)
210  FORMAT(0,15X,'TOTAL WING CL=',F10.6,5X,'AT MACH=',F10.6,'AND SLE
1=,F6.2,'DEGREES',//)
211  WRITE(6,211)CRM
      FORMAT(0,1,ROLLING MOM. COEFF.=',F10.6)
      CMA(N)=0.0
DO 212 I=1,NZ
  CMA(N)=CMA(N)+AR/CMAC*H*ALPHA(I)*(((XAL1)+XB(I))/2.0)-XMAC)
212  CONTINUE
213  WRITE(6,213)CMA(N)
      FORMAT(0,1,CM-ALPHA=',F10.6)
      CMCL=CMA(N)/CLT(N)
      WRITE(6,245)CMCL
      BMACH(N+1)=BMACH(N)+0.1
240  CONTINUE
241  WRITE(6,241)DEG
      FORMAT(1,///,T49,'CL-ALPHA VS. MACH.',3X,'AT ',F6.2,'LEADING ED
1GE SWEEP',///)
      CALL UTPLT(BMACH,CLT,10,RANGE,2,0)
      WRITE(6,242)DEG
242  FORMAT(1,///,T49,'CM-ALPHA VS. MACH.',3X,'AT ',F6.2,'LEADING ED
1GE SWEEP',///)

```



```

WRITE(6,213)CMA(5)
CALL UTPLLOT(BMACH,CMA,10,RANGE1,2,0)
FORMAT('0',15X,'DCM/DCL=',F10.6//)
245 SLE=SLE+0.17453292
DEG=DEG+10.0
250 CONTINUE
END

*
*
* THIS PROGRAM WAS DESIGNED TO OBTAIN THE ROLLING MOMENT DUE TO AILERON
DEFLECTION, (DCL)/(CDDA), FOR ARBITRARY PLANFORMS AT A MACH NUMBER OF 0.5.
IMPLICIT REAL*8(A-H,O-Z)
COMMON/C1/AR,TR,SLE,R,NC,NS,CMAC,XMAC,YMAC,YA(100),YB(100),YC(100)
1 YAI(100),YBI(100),XA(100),XB(100),XC(100),AREA,BMACH
COMMON/C2/AS(20,20),AA(20,20)
COMMON/C3/EA(6),XC4(5),C(5),CP(20),ALPHA(20),CL(5),RHO,VT,DX(5,20)
COMMON/C4/S(20,20),Q,TH(4,4),EI(10),GJ(10)
DIMENSION CLC(10),IHEFA(13),B(13,13),J(23,20),CLC1(10)
R=0.0
IDENTIFY THE PLANFORM BY READING IN THE NUMBER OF CHORDWISE AND SPANWISE
STATIONS, THE ASPECT RATIO, THE TAPER RATIO, AND THE STIFFNESS PROPERTIES.
1 FORMAT(2I3,2F10.6)
READ(5,2)(EI(1),I=1,NS)
2 FORMAT(8F10.6)
ANC=NC
NS2=2**NS
NSP1=NS+1
NSP2=NS+2
NZ=NC*NS
NC2=2**NC
NC3=3**NC
NC4=4**NC
PI=3.141592653
READ IN THE AIR DENSITY CORRESPONDING TO THE DESIRED ALTITUDE.
3 FORMAT(F10.6)
X=0.175
SLE=DATAN(X)
DEG=SLE*57.3
BMACH=0.5
Q=0.0
VT=BMACH*1116.89
CALL GEOM
CALL AERC
CALL STRUCT

```



```

DO 220 N=1,19
INPUT THE ANGLE OF ATTACK DISTRIBUTION FOR ALPHA = 0 EVERYWHERE EXCEPT
AT THE ALLERON LOCATION WHERE ALPHA = 1.0.
DO 10 I=1,NZ
ALPHA(I)=0.0
10 CONTINUE
ALPHA(16)=1.0
ALPHA(20)=1.0
DO 15 I=1,NZ
DO 15 J=1,NZ
15 U(I,J)=AA(I,J)-Q*S(I,J)
ELU AND SLVB SOLVE THE EQUATION : (AA-Q*S)*(L/Q) = ALPHA .
CALL ELU(U,NZ,20)
CALL SLVB(U,NZ,20,ALPHA)
WRITE(6,20)
20 FORMAT(1.0,10X,'PROGRAM CHECK OF LOAD DISTRIBUTION:',//,15X,
1,ALPHA=1.0,AND',//,3X,'STA',4X,'ETA',8X,'X',5X,'DEL(L/Q)',//)
DO 30 I=1,NZ
XC1=0.5*(XA(I)+XB(I))
WRITE(6,21)I,YC(I),XC1,ALPHA(I)
21 FORMAT(2X,13,3F10.6)
30 CONTINUE
NOW A COLLOCATION TECHNIQUE IS SET UP TO INTEGRATE THE LIFT DISTRIBUTION TO
OBTAIN THE ROLLING MOMENT COEFFICIENT. THE THETA'S ARE THE COLLOCATION POINTS.
DO 40 I=1,NS
THETA(I)=DARCOS(YC(K))
NC1=(I-1)*NC+1
NC1=I*NC
IF(I.EQ.NS) GO TO 31
K=K+NC
31 CLC(I)=0.0
DO 40 J=NC1,NCI
CLC(I)=CLC(I)+ALPHA(J)
40 CONTINUE
K=I
DO 41 I=NSPI,NS2
THETA(I)=DARCOS(-YC(K))
K=K+NC
41 CONTINUE
DO 70 I=1,NS
CLC(I)=CLC(I)/C(I)
70 CONTINUE
WRITE(6,111)
111 FORMAT(//,15X,'SECTION LIFT COEFFICIENTS',//,4X,'STA',5X,'CL',//)
112 WRITE(6,112)I,CL(I),I=1,NS)
FORMAT(5X,11,3X,F10.6)
CAVE=2.0/AR

```





```

DO 200 I=1,NS2
DO 200 J=1,NS2
AJ=J
CONTINUE
DO 201 I=1,NS
CLC1(I)=CLC(NSPI-I)
CONTINUE
DO 202 I=NSPI,NS2
CLC1(I)=-CLC(1-NS)
CONTINUE
NOW ELU AND SLVB ARE USED TO SOLVE FOR THE FOURIER COEFFICIENTS
CALL ELU(B,NS2,10)
CALL SLVB(B,NS2,10,CLC1)
WRITE(6,203)(I,CLC1(I),I=1,NS2)
203 FORMAT(15X,B(1),CLC1(1),=,F10.6)
CRM=PI/16.0*CLC1(2)
WRITE(6,211)CRM,Q
211 FORMAT(6,'',ROLLING MOM. COEFF.=,F10.6,5X,'@ Q=,F10.6)
Q=Q+1.0
220 CONTINUE
END

```

```

*
* THIS PROGRAM WAS DESIGNED TO OBTAIN THE DAMPING IN ROLL DERIVATIVE,
* (DCL)/(DPB/2V), FOR ARBITRARY PLANKFORMS AT A MACH NUMBER OF 0.5.
* IMPLICIT REAL*8(A-H,O-Z)
* COMMON/CL/AR,TR,SLE,R,NC,NS,CMAC,XMAC,YMAC,YA(100),YB(100),YC(100)
* 1,YAI(100),YBI(100),XA(100),XB(100),XC(100),AREA,BWACH
* COMMON/CC/AS(20,20),AA(20,20)
* COMMON/CC3/EA(9),XC4(5),C(5),CP(20),ALPHA(20),CL(5),RHO,VT,DX(5,20)
* COMMON/CC4/S(20,20),Q,TH(4,4),EI(10),GJ(10)
* DIMENSION CLC(10),THETA(10),B(10,10),U(20,20),CLC1(10)
R=J,J
IDENTIFY THE PLANKFORM BY READING IN THE NUMBER OF CHORDWISE AND SPANWISE
STATIONS, THE ASPECT RATIO, THE TAPER RATIO, AND THE STIFFNESS PROPERTIES.
1 READ(5,1)(NC,NS,AR,TR)
FORMAT(2I3,2F10.6)
2 READ(5,2)(EI(I),I=1,NS)
READ(5,2)(GJ(I),I=1,NS)
FORMAT(8F10.6)
ANC=NC
NS2=2*NS
NSPI=NS+1
NSP2=NS+2
NZ=NC*NS
NC2=2*NC

```



```

NC3=3*NC
NC4=4*NC
PI=3.141592653
READ IN THE AIR DENSITY CORRESPONDING TO THE DESIRED ALTITUDE.
3  FORMAT(F10.6)
X=0.175
SLE=DATAN(X)
DEG=SLF*57.3
BMACH=0.5
Q=0.0
VT=0MACH*1116.89
CALL GFCM
CALL AERO
CALL STRUCI
DO 220 N=1,19
  INPUT THE ANGLE OF ATTACK DISTRIBUTION FOR ALPHA = 0 AT THE ROOT AND
  ALPHA = 1.0 AT THE TIP.
  DO 10 I=1,NC
    ALPHA(I)=0.1
    ALPHA(I+NC2)=0.3
    ALPHA(I+NC3)=0.5
    ALPHA(I+NC4)=0.7
    ALPHA(I+NC4)=0.9
  10 CONTINUE
  DO 15 I=1,NZ
    DO 15 J=1,NZ
      15 U(I,J)=AA(I,J)-Q*S(I,J)
      ELU AND SLVB SOLVE THE EQUATION : (AA-Q*S)*(L/Q) = ALPHA
      CALL ELU(U,NZ,20)
      CALL SLVB(U,NZ,20,ALPHA)
      WRITE(6,20),LOX,PRGRAM,CHECK OF LCAD DISTRIBUTION:'.//',15X,
20 1,ALPHA=1.0,RAD, '//,3X,'STA',4X,'ETA',8X,'X',5X,'DEL(L/Q)',,/,)
      DC 30 I=1,NZ
      XC1=0.5*(XA(I)+XB(I))
      WRITE(6,21),YC(I),XC1,ALPHA(I)
21  FORMAT(2X,I3,3F10.6)
30 CONTINUE
NCW A COLLOCATION TECHNIQUE IS SET UP TO INTEGRATE THE LIFT DISTRIBUTION TO
OBTAIN THE ROLLING MOMENT COEFFICIENT. THE THETAS ARE THE COLLOCATION POINTS.
K=NZ-NC+1
DO 40 I=1,NS
  THETA(I)=DARCOS(YC(K))
  NC1=(I-1)*NC+1
  NC2=I*NC
  IF(1.EQ.NS) GO TO 31
  K=K-NC

```



```

31 CLC(I)=0.0
   DO 40 J=NC1,NCI
   CLC(I)=CLC(I)+ALPHA(J)
40 CONTINUE
   K=1
   DO 41 I=NSP1,NS2
   THETA(I)=DARCOS(-YC(K))
   K=K+NC
41 CONTINUE
   DO 70 I=1,NS
   CL(I)=CLC(I)/C(I)
70 CONTINUE
   WRITE(6,111)
111 FORMAT(//,15X,'SECTION LIFT COEFFICIENTS',//,4X,'STA',5X,'CL',//)
112 WRITE(6,112)(I,CL(I),I=1,NS)
   FORMAT(5X,11,3X,F10.6)
   CAVE=2.0/AR
   DO 200 I=1,NS2
   DO 200 J=1,NS2
   AJ=J
   P(I,J)=DSIN(AJ*THETA(I))
200 CONTINUE
   DO 201 I=1,NS
   CLC(I)=CL(NSP1-I)
201 CONTINUE
   DO 202 I=NSP1,NS2
   CLC(I)=-CLC(I-NS)
202 CONTINUE
   NOW ELU AND SLVB ARE USED TO SOLVE FOR THE FOURIER COEFFICIENTS
   CALL ELU(B,NS2,10)
   CALL SLVB(B,NS2,10,CLC1)
   WRITE(6,203)(I,CLC1(I),I=1,NS2)
203 FORMAT(15X,8(,12,))=,F10.6)
   CRM=PI/16.0*CLC1(2)
   WRITE(6,211)CRM,Q
211 FORMAT(0,'ROLLING MOM. COEFF.=',F10.6,5X,'@ Q=',F10.6)
   Q=Q+1.0
220 CONTINUE
220 END

```

SUBROUTINE GEOM  
THIS SUBROUTINE IS USED TO DEFINE THE LOCATION OF THE HORSESHOE VORTICES  
AND THEIR CONTROL POINTS ALL OVER THE PLANEFORM. OTHER SIMPLE GEOMETRY  
PROBLEMS ARE ALSO WORKED OUT.  
IMPLICIT REAL\*8(A-H,O-Z)  
COMMON/C1/AR,TR,SLE,P,NC,NS,CMAC,XMAC,YMAC,YA(100),YB(100),YC(100)  
1,YA(100),YB(100),XA(100),XB(100),XC(100),AREA,BMACH



```

COMMON/C3/EA(9),XC4(5),C(5),CP(20),ALPHA(20),CL(5),RHO,VT,DX(5,20)
CR=4./((1.+TR)*AR)
CT=TR*CR
AREA=4./AR
TSL=DTAN(SLE)
CMAC=(2./3.)*(CT+CR-(CT*CR/(CT+CR)))
YMAC=1./3.)*((CR+2.*CT)/(CR+CT))
XMAC=YMAC*TSL+0.25*CMAC
ANS=MS
ANC=NC
DO 20 I=1,NS
  AI=1
  YAI=((AI-1.)*(1.-R))/(ANS+R)
  YBI=(AI*(1.-R))/ANS+R
  YCI=0.5*(YAI+YBI)
  NC1=(1-1)*NC+1
  NC2=1*NC
  CA=CR-YAI*(CR-CT)
  CB=CR-YBI*(CR-CT)
  CC=0.5*(CA+CB)
  AJ=0.0
  IF(R.EQ.0.0) GO TO 12
  YA2=R**2/YAI
  YB2=R**2/YBI
  GO TO 11
12 YA2=0.0
  YB2=0.0
11 DO 20 J=NC1,NC2
  AJ=AJ+1.0
  XA(J)=YAI*TSL+CA*(AJ-0.75)/ANC
  XB(J)=YBI*TSL+CB*(AJ-0.75)/ANC
  XC(J)=YCI*TSL+CC*(AJ-0.25)/ANC
  YB(J)=YBI
  YC(J)=YCI
  YAI(J)=YAI
  YBI(J)=YBI
20 CONTINUE
WRITE(6,21) AR,TR,TSL,AREA,CT,CMAC,XMAC,YMAC,R,CR
21 FORMAT(1,5X,AR=,F10.6,5X,TR=,F10.6,4X,TSL=,F10.6,3X,AREA=,
1,F10.6,5X,CT=,F10.6,7,4X,MAC=,F10.6,3X,XMAC=,F10.6,3X,YMAC
1=,F10.6,6X,R=,F10.6,5X,CR=,F10.6,7)
NZ=NC*NS
C C(I) IS THE CHORD LENGTH AT SPANWISE STA. I, I=1,NS
C DX(I,J) IS STRMWISE DIST FROM EA(I) TO LOCAL C/4 PT. FOR STA. J, J=1,NZ
DO 8 I=1,NS
  C(I)=CR*(1.0-(1.0-TR)*YC(J))

```





```

      J=J+4
      8 CONTINUE
      NSP1=NS+1
      NSP2=NS+2
      C COMPUTE THE E. A. LOCATION
      J=1
      EA(I)=0.35*CR
      DO 29 I=2, NSP1
      EA(I)=0.35*(C(I-1)+TSL*YC(J)
      J=J+4
      29 CONTINUE
      EAINSP2)=0.35*CT+TSL
      LOCAL C/4 PTS FOR EACH SECTION
      J=1
      DO 30 I=1, NS
      XC4(I)=C(I)/4.0+TSL*YC(J)
      J=J+4
      30 CONTINUE
      DX(I,J)=STREAMWISE DISTANCE BETWEEN LOCAL C/4 PIAT STATION J,
      TO THE E. A. PT AT STATION I.
      DO 32 I=1, NS
      DO 31 J=1, NZ
      DX(I,J)=EA(I+1)-(XA(J)+XB(J))/2.0
      31 CONTINUE
      32 RETURN
      END

```

```

SUBROUTINE AERO
THIS SUBROUTINE IS USED TO OBTAIN THE AERODYNAMIC INFLUENCE COEFFICIENT
MATRIX FOR BOTH THE SYMMETRIC AND ANTI-SYMMETRIC LOAD DISTRIBUTIONS.
AA CORRESPONDS TO THE ANTI-SYMMETRIC DISTRIBUTION, WHILE AS CORRESPONDS
TO THE SYMMETRIC DISTRIBUTION.
COMMON/C1/AR,TR,SLE,R,NC,NS,CMAC,XMAC,YMAC,YAL(100),YB(100),YC(100)
1 YAL(100),YB(100),XA(100),XB(100),XC(100),AREA,BMACH
COMMON/C2/AS(20,20),AA(20,20)
BETA2=1.0/41.0-BMACH**2
BETA1=DSQRT(BETA2)
NCNST=0.125/3.141592654
NZ=NC*NS
DO 31 I=1, NZ
DO 30 J=1, NZ
RA1=DSQRT((YC(I)-YA(J))**2+BETA2*((XC(I)-XA(J))**2))
RA2=DSQRT((YC(I)+YA(J))**2+BETA2*((XC(I)-XA(J))**2))
RB1=DSQRT((YC(I)-YB(J))**2+BETA2*((XC(I)-XB(J))**2))
RB2=DSQRT((YC(I)+YB(J))**2+BETA2*((XC(I)-XB(J))**2))
SNT1=1/(XC(I)-XA(J))/(RA1)*BETA1

```



```

CST1=(YC(I)-YA(J))/RA1
SNT2=((XC(I)-XA(J))/RA2)*BETA1
CST2=((YC(I)+YA(J))/RA2
SNP1=((XC(I)-XB(J))/RB1)*BETA1
CSP1=((YC(I)-YB(J))/RB1
CNP2=((XC(I)-XB(J))/RB2)*BETA1
CSP2=((YC(I)+YB(J))/RB2
HAB=DSQR((YB(J)-YA(J))*2+BETA2*((XB(J)-XA(J))*2))
SNG1=((XB(J)-XA(J))/RAB)*BETA1
SNG2=-1.0*SNG1
CSG1=(YB(J)-YA(J))/RAB
CSG2=CSG1
CSA1=CST1*CSG1+SNT1*SNG1
SNA1=SNT1*CSG1-CST1*SNG1
CSB1=CSP1*CSG1+SNP1*SNG1
CSA2=CST2*CSG2+SNT2*SNG2
SNA2=CSP2*CSG2+SNP2*SNG2
AL1=(1.0+SNT1)/(YC(I)-YA(J))
AL2=(1.0+SNT2)/(YC(I)+YA(J))
AR2=(1.0+SNT2)/(YC(I)+YB(J))
ASA1=DABS(SNA1)
AA2=DABS(SNA2)
IF(ASA1.LT.0.0001) GO TO 10
GU TO 11
AR1=(1.0*(R/YC(I))*2)*(CSA1-CSB1)/(SNA1*RA1)
10 AR1=0.0
11 IF(ASA2.LT.0.0001) GO TO 12
12 AR2=(1.0*(R/YC(I))*2)*(CSA2-CSB2)/(SNA2*RA2)
GU TO 13
13 AR2=0.0
ARW=AL1-AR1+AB1
ALW=AL2-AR2+AB2
AS(I,J)=CCNST*(ARW-ALW)
AA(I,J)=CCNST*(ARW+ALW)
30 CCNTINUE
31 RETURN
END

```

SUBROUTINE ELU TRI-DIAGONALIZES THE INPUT SQUARE MATRIX FOR SOLUTION.



```

SUBROUTINE ELU(A,N,NC)
IMPLICIT REAL*8(A-H,O-Z)
DIMENSION A(ND,NC)
NM1=N-1
DO 100 K=1,NM1
  KP1=K+1
  DO 100 I=KP1,N
    G=-A(I,K)/A(K,K)
    A(I,K)=G
    DO 100 J=KP1,N
      100 A(I,J)=A(I,J)+G*A(K,J)
    RETURN
  END

```

SUBROUTINE SLVB SOLVES THE TRI-DIAGONALIZED MATRIX FROM ELU BY THE BACK SUBSTITUTION METHOD.

```

SUBROUTINE SLVB(A,N,ND,B)
IMPLICIT REAL*8(A-H,O-Z)
DIMENSION A(ND,ND),B(ND)
NM1=N-1
NP1=N+1
DO 100 K=1,NM1
  KP1=K+1
  DO 100 I=KP1,N
    B(I)=B(I)+A(I,K)*B(K)
    100 B(I)=B(I)/A(N,N)
  DO 300 K=2,N
    I=NP1-K
    JI=I+1
    DO 200 J=JI,N
      200 B(I)=B(I)-A(I,J)*B(J)
      300 B(I)=B(I)/A(I,I)
    RETURN
  END

```

SUBROUTINE STRUCT COMPUTES THE STRUCTURAL INFLUENCE COEFFICIENT MATRIX FOR THE INPUT PLANFORM. THE RESULTING MATRIX IS COUPLED IN BOTH BENDING AND TORSION.



```

SUBROUTINE STRUC1
  IMPLICIT REAL*8(A-H,M,O-Z)
  COMMON/C1/AR,TR,SLE,R,NC,NS,CMAC,XMAC,YMAC,YA(100),YB(100),YC(100)
  1,YA(100),YB(100),XA(100),XB(100),XC(100),CP(100),ALPHA(20),CL(5),RHO,VT,DX(5,20)
  COMMON/C3/EA(9),XC4(5),C(5),C(5),TH(4,4),FI(10),GJ(10)
  COMMON/C4/S(20,20),Q,TH(4,4),FI(10),GJ(10)
  DIMENSION HEI(10,10),GJ1(10,10),MI(20,5),FI(20,5),THETA(20,20),
  1B(20,20),AM(20,20),VV(5,20),UU(5,20)
  DIMENSION SEEA(10),SSEA(10),CSEA(10),DL(5,5),SL(5,5),V(5,20),U(5,20)
  1),X(20),Y(20)
  H=0.5/HN
  F2=H**2
  NC2=2*NC
  NC3=3*NC
  NC4=4*NC
  NCPI1=NC+1
  NCPI2=NC2+1
  NCPI3=NC3+1
  NC4PI1=NC4+1
  NSM2=NS-2
  NSM3=NS-3
  NZ=NC*NS
  NSM1=NS-1
  NSPI1=NS+1

```

THE AM MATRIX CORRESPONDS TO THE BENDING MOMENTS, AND THE B MATRIX  
CORRESPONDS TO THE TORSIONAL MOMENTS.

```
PI=3.141592653
```

```
DO 140 I=1,NS
DO 140 J=1,NZ
```

```
140 AM(I,J)=0.0
```

```
DO 150 I=1,NC
B(1,I)=DX(1,I)
```

```
150 CC=NTINUE
```

```
DO 151 I=1,NCPI1,NZ
```

```
151 B(1,I)=2.0*DX(1,I)
```

```
DO 152 I=1,NCPI1,NC2
```

```
152 B(2,I)=CX(2,I)
```

```
DO 153 I=1,NC2PI1,NZ
```

```
153 B(2,I)=2.0*DX(2,I)
```

```
DO 154 I=1,NC2PI1,NC3
```

```
154 B(3,I)=DX(3,I)
```

```
DO 155 I=1,NC3PI1,NZ
```

```
155 B(3,I)=2.0*DX(3,I)
```

```
DO 156 I=1,NC3PI1,NC4
```

```
156 B(4,I)=DX(4,I)
```

```
DO 157 I=1,NC4PI1,NZ
```





```

157 B(4,I)=2.0*DX(4,I)
158 DO 158 I=NC4P1,NZ
159 K=1
160 L=NC
161 DO 180 I=1,NS
162 DO 179 J=K,L
163 AM(I,J)=0.5*H
164 K=K+NC
165 L=L+NC
166 CONTINUE
167 K=NCPI
168 L=NC2
169 DO 182 I=1,NSM1
170 DO 181 J=K,L
171 AM(I,J)=4.0*H
172 K=K+NC
173 L=L+NC
174 CONTINUE
175 K=NC2PI
176 L=NC3
177 DO 184 I=1,NSM2
178 DO 183 J=K,L
179 AM(I,J)=8.0*H
180 K=K+NC
181 L=L+NC
182 CONTINUE
183 K=NC3PI
184 L=NC4
185 DO 186 I=1,NSM3
186 DO 185 J=K,L
187 AM(I,J)=12.0*H
188 K=K+NC
189 L=L+NC
190 CONTINUE
191 DO 187 I=NC4P1,NZ
192 AM(I,I)=16.0*H
193 SEA IS THE SWEEP OF THE ELASTIC AXIS.
194 SEA(I)=DATAN((EA(3)-EA(1))/3.0*H)
195 DO 220 I=2,NSM1
196 SEA(I)=DATAN((EA(I+2)-EA(I))/4.0*H)
197 CONTINUE
198 SEAIN(I)=DATAN((EA(NS+2)-EA(NS))/3.0*H)
199 WRITE(6,221)IOX,'SWEEP OF E. A. IN RADDS.',//,4X,'STA',5X,'SEA',//
200 FORMAT(6,222)I,SEA(I),I=1,NS)
201 WRITE(6,222)I,5X,F10.6)
202 FORMAT(5X,I,5X,F10.6)
203 SSEA IS THE SIN OF THE SWEEP OF THE ELASTIC AXIS, AND CSEA IS THE COS.

```



```

230      DO 230 I=1,NS
          SSEA(I)=DSIN(SEA(I))
          CONTINUE
230      DO 240 I=1,NS
          CSEA(I)=DCOS(SEA(I))
          CONTINUE
240      DO 250 I=1,NS
          CL(I,J)=0.0
          SL(I,J)=0.0
          CONTINUE
250      DO 260 I=1,NS
          DL(I,I)=CSEA(I)
          SL(I,I)=SSEA(I)
          CONTINUE
260      DO 270 I=1,NS
          V(I,J)=0.0
          WV(I,J)=0.0
          UV(I,J)=0.0
          CONTINUE
270      DO 280 I=1,NS
          DO 280 J=1,NZ
          DO 280 K=1,NS
          V(I,J)=DL(I,K)*B(K,J)+V(I,J)
          WV(I,J)=SL(I,K)*AM(K,J)+WV(I,J)
          UV(I,J)=SL(I,K)*B(K,J)+UV(I,J)
          CCNT INUE
280      DO 290 I=1,NS
          DO 290 J=1,NZ
          B(I,J)=V(I,J)+U(I,J)
          WV(I,J)=WV(I,J)-UV(I,J)
          CONTINUE
290      DO 310 I=1,NS
          DO 310 J=1,NS
          FEI(I,J)=0.0
          GJI(I,J)=0.0
          CONTINUE
310      DO 320 I=1,NS
          HEI(I,I)=6.25/(EI(I)*CSEA(I))
          GJI(I,I)=6.25/(GJ(I)*CSEA(I))
          CONTINUE
320      DO 330 I=1,NS
          DO 330 J=1,NZ
          U(I,J)=0.0
          VI(I,J)=0.0
          CONTINUE
330      DO 340 I=1,NS

```



```

DO 340 J=1,NZ
DO 340 K=1,NS
V(I,J)=HEI(I,K)*AM(K,J)+V(I,J)
U(I,J)=GJ(I,K)*B(K,J)+U(I,J)
340 CONTINUE
DO 350 I=1,NZ
DO 350 J=1,NS
MI(I,J)=0.0
TI(I,J)=0.0
350 CONTINUE
DO 360 I=1,NS
MI(I,I)=-SEA(I)/2.0
TI(I,I)=CSEA(I)/2.0
360 K=2
DO 380 I=1,NSM1
DO 370 J=K,NS
MI(I,J)=-SEA(J)
TI(I,J)=CSEA(J)
370 CONTINUE
380 K=K+1
DO 385 I=1,NZ
DO 385 J=1,NZ
AM(I,J)=0.0
BI(I,J)=0.0
385 NK1=1
NK2=NC
DO 400 I=1,NS
DO 390 J=1,NS
DO 390 K=NK1,NK2
AM(K,J)=MI(I,J)
B(K,J)=TI(I,J)
390 CONTINUE
NK1=NK2+1
NK2=NC+NC
400 CONTINUE
DO 410 I=1,NZ
DO 410 J=1,NS
MI(I,J)=AM(I,J)
TI(I,J)=BI(I,J)
410 CONTINUE
DO 420 I=1,NZ
DO 420 J=1,NS
BI(I,J)=0.0
AM(I,J)=0.0
DO 430 I=1,NZ
DO 430 J=1,NS
BI(I,J)=MI(I,K)*V(K,J)+B(I,J)
430 AM(I,J)=TI(I,K)*U(K,J)+AM(I,J)

```



```

DO 440 I=1,NZ
DO 440 J=1,NZ
440 B(I,J)=B(I,J)+AM(I,J)
DO 500 I=1,NZ
DO 500 J=1,NZ
500 S(I,J)=2.0*H2*B(I,J)
RETURN
END

```





## REFERENCES

1. Gray, W. L. and Schenk, K.M., "A method for Calculating the Subsonic Steady-State Loading on an Airplane with a Wing of Arbitrary Planform and Stiffness," NACA TN 3030, December 1953.
2. Kuethe, A. M. and Schetzer, J. D., Foundations of Aerodynamics, John Wiley and Sons, 1958.
3. Bisplinghoff, R.L., Ashley, H., Halfman, R. L., Aeroelasticity, Addison-Wesley, 1957.
4. Belotserkovskii, S. M., The Theory of Thin Wings in Subsonic Flow, Plenum Press, 1967.
5. Etkin, B., Dynamics of Flight, John Wiley and Sons, 1959.
6. Ashley, H. and Landahl, M., Aerodynamics of Wings and Bodies, Addison-Wesley, 1965.



# INITIAL DISTRIBUTION LIST

|   | No. Copies |
|---|------------|
| 1. Defense Documentation Center<br>Cameron Station<br>Alexandria, Virginia 22314  | 2          |
| 2. Library, Code 0212<br>Naval Postgraduate School<br>Monterey, California 93940  | 2          |
| 3. Professor L. V. Schmidt, Code 57Sx<br>Department of Aeronautics<br>Naval Postgraduate School<br>Monterey, California 93940 | 1          |
| 4. LT Larry G. Pearson<br>VF-124<br>NAS Miramar, California 92145   | 1          |
| 5. Chairman, Department of Aeronautics<br>Naval Postgraduate School<br>Monterey, California 93940                             | 1          |
| 6. Mr. H. Andrews<br>NAIR 5301<br>Department of the Navy<br>Washington, D. C. 20360   | 1          |



## DOCUMENT CONTROL DATA - R &amp; D

(Security classification of title, body of abstract and indexing annotation must be entered when the overall report is classified)

|   |   |   |  |
|---|---|---|--|
| ORIGINATING ACTIVITY (Corporate author)   |   | 2a. REPORT SECURITY CLASSIFICATION                      |  |
| Naval Postgraduate School<br>Monterey, California 93940   |   | Unclassified  |  |
| REPORT TITLE  |   | 2b. GROUP   |  |
| Subsonic Lifting Surface Analysis with Static Aeroelastic Effects   |   |   |  |
| 1. DESCRIPTIVE NOTES (Type of report and inclusive dates)<br>Master's Thesis; June 1972   |   |   |  |
| 3. AUTHOR(S) (First name, middle initial, last name)<br>Larry Glen Pearson  |   |   |  |
| 4. REPORT DATE  | 7a. TOTAL NO. OF PAGES  | 7b. NO. OF REFS   |  |
| June 1972   | 74  | 6   |  |
| 6a. CONTRACT OR GRANT NO.   | 9a. ORIGINATOR'S REPORT NUMBER(S)   |   |  |
| b. PROJECT NO.  |   |   |  |
| c.  | 9b. OTHER REPORT NO(S) (Any other numbers that may be assigned this report) |   |  |
| d.  |   |   |  |
| 10. DISTRIBUTION STATEMENT<br>Approved for public release; distribution limited.  |   |   |  |
| 11. SUPPLEMENTARY NOTES   |   | 12. SPONSORING MILITARY ACTIVITY                        |  |
|   |   | Naval Postgraduate School<br>Monterey, California 93940 |  |
| 13. ABSTRACT<br>A computer program was coded to obtain static aeroelastic effects on simple planforms through the use of subsonic lifting surface theory. The program was divided into two major technical areas, aerodynamic and structural, with matrix notation used to indicate the influence of each in the final aerodynamic loading distribution. Several typical stability derivatives were then obtained to make an accurate stability and control analysis on the desired planform. |   |   |  |



| KEY WORDS                | LINK A |    | LINK B |    | LINK C |    |
|--------------------------|--------|----|--------|----|--------|----|
|                          | ROLE   | WT | ROLE   | WT | ROLE   | WT |
| Lifting surface          |        |    |        |    |        |    |
| Aeroelastic              |        |    |        |    |        |    |
| Stability and control    |        |    |        |    |        |    |
| Subsonic compressibility |        |    |        |    |        |    |
| Low aspect ratio         |        |    |        |    |        |    |
| Swept wings              |        |    |        |    |        |    |









11 JUN 74

20486

14 NOV 74

23548

1 JUN 76

23355

10 DEC 80

24049

26018

134717

Thesis

P313

Pearson

c.1

Subsonic lifting  
surface analysis with  
static aeroelastic

11 JUN 74 effects.

20486

23548

1 JUN 76

23355

10 DEC 80

24049

26018

th

134717

Thesis

P313

Pearson

c.1

Subsonic lifting  
surface analysis with  
static aeroelastic  
effects.

thesP313

Subsonic lifting surface analysis with s



3 2768 001 97904 0

DUDLEY KNOX LIBRARY